JOURNAL OF NEUROPHYSIOLOGY
Vol. 76, No. 2, August 1996. *Printed in U.S.A.*

Cochlear Nerve Activity After Intense Sound Exposure in Neonatal Chicks

JAMES C. SAUNDERS, DARYL E. DOAN, CHRISTOPHER P. POJE, AND KIMBERLY A. FISHER
Department of Otorhinolaryngology—Head and Neck Surgery and Department of Bioengineering, University of Pennsylvania; and Division of Otolaryngology, Children's Hospital of Philadelphia, Philadelphia, Pennsylvania 19104

SUMMARY AND CONCLUSIONS

1. Single-neuron behavior in the cochlear nerve of neonatal (3-day-old) chicks was examined after exposure to a 120-dB SPL pure tone (0.9 kHz) for 48 h. Exposed animals were tested after 0 days or 12 days of recovery. Nonexposed chicks, age-matched to the exposed animals, formed two control groups.

2. Spectral response plots were obtained from each cell. These plots described the neuron discharge rates in response to 1,767 tone burst stimuli, each with a unique frequency-intensity combination. The tone bursts were presented at frequencies between 0.1 and 4.5 kHz and for intensities between 0 and 100 dB SPL. From these plots the characteristic frequency (CF), CF threshold, and sharpness of tuning ($Q_{10\,dB}$) were derived for each cell. Frequency response–area functions at selected stimulus levels and rate-intensity functions at the CF were also constructed from the spectral response plots. In addition, spontaneous activity was determined. Data were obtained from 903 cells.

3. Neuron activity in the control cells revealed no differences between CF thresholds, $Q_{10\,dB}$, or spontaneous activity in the two age groups. However, age differences at all frequencies were noted in the rate-intensity functions.

4. A frequency-dependent loss in CF threshold was observed in the 0-day recovered cells. The threshold shift (relative to age-matched control cells) was 55–65 dB between 0.8 and 1.5 kHz, but only 10–15 dB between 0.1–0.4 kHz and 2.5–3.5 kHz. The exposed cells showed no loss in frequency selectivity ($Q_{10\,dB}$) at <0.5 kHz, whereas above this frequency an increasing deterioration in tuning was noted. Spontaneous activity in the 0-day cells was suppressed across the entire range of CFs. The rate-intensity function of exposed cells had a steeper growth rate than that of control cells.

5. At 12 days of recovery, CF threshold, $Q_{10\,dB}$, and spontaneous activity all recovered to the levels exhibited by age-matched control cells. However, the rate-intensity function for cells with CFs between 0.8 and 1.0 kHz showed abnormal growth and higher discharge rates at saturation than the control cells. Outside of this frequency range the rate-intensity functions of control and exposed cells were similar to each other.

6. Recovery of function in the sound-damaged chick ear is accompanied by almost complete repair of the basilar papilla. The tectorial membrane, however, retains a major defect and only the lower layer of this membrane regenerates. An important observation in this presentation was the abnormal rate-intensity functions (in the 12-day recovered cells) reported for frequencies served by that region of the sensory epithelium where the tectorial membrane defect was found. This observation may be related to sustained structural damage to the short hair cell region of the papilla and/or alterations in the efferent control of papilla function mediated by the short hair cells.

INTRODUCTION

Acoustic damage to the chick cochlea has become an important model for studying the processes of functional recovery in the auditory system. Intense sound creates so-called "patch and stripe" lesions on the surface of the sensory epithelium (Cotanche 1987a). The patch is a circumscribed region of damage located on the abneural side of the basilar papilla at the appropriate tonotopic location for the exposure frequency. Within the patch there is a 30–35% loss of short hair cells (Cotanche 1987a; Henry et al. 1988; Marsh et al. 1990), destruction of the tectorial membrane (Cotanche 1987b), and severe changes in the cellular organization of the sensory surface (Raphael 1993; Saunders et al. 1992). The stripe lesion is a narrow band of intermediate hair cell loss basal to the patch and in the approximate middle of the papilla. The tectorial membrane above the stripe remains intact. Other aspects of papilla damage have been summarized elsewhere (Cotanche et al. 1994). Within 12 days postexposure, new hair cells emerge to repopulate the sensory surface, the lower "honeycomb" layer of the tectorial membrane regenerates, and the organization of the sensory surface returns to a more normal appearance (Cotanche 1987a,b; Henry et al. 1988; Raphael 1993). In addition, the stereocilia bundles on the newly regenerated hair cells also appear to achieve a correct orientation (Cotanche and Corwin 1991). Structural recovery, however, is incomplete. The new hair cells do not replace all those lost to overstimulation (Marsh et al. 1990), and the upper layer of the tectorial membrane does not return (Adler et al. 1993; Cotanche 1987b). Moreover, the hexagonal mosaic of the hair cell field never completely returns in the repaired ear (Cotanche 1987a; Henry et al. 1988).

Changes in the innervation patterns of the patch and stripe lesion are not well understood in the chick, but have been studied in greater detail in the quail. The innervation of quail hair cells that survive the exposure appears normal (Ryals et al. 1992). There is also evidence that the afferent and efferent synaptic endings return on regenerated tall and short hair cells within 10 days postexposure (Ryals and Westbrook 1994). It also appears that the quail undergoes a progressive loss for many months after the exposure in the number of cochlear ganglion cells and nerve fibers (Ryals et al. 1989).

Field-evoked potentials or single-cell recordings from chick nucleus magnocellularis at 0 days of recovery showed a 50- to 55-dB threshold shift and a 45–55% reduction in the frequency selectivity of tuning curves (Cohen and Saunders 1993; McFadden and Saunders 1989; Saunders et al. 1993). In addition, the neural representation of stimulus intensity for frequencies coded within the boundaries of the patch lesion exhibited abnormally rapid growth in activity as the stimulus level rose (Cohen and Saunders 1993; Pugli-

ano et al. 1993a). Within 3 days postexposure, there was a significant degree of functional recovery that was nearly complete by 12–24 days postexposure (Adler et al. 1993; McFadden and Saunders 1989; Pugliano et al. 1993a,b). Finally, the endocochlear potential also showed severe loss immediately after the exposure, and then complete recovery within 3 days postexposure (Poje et al. 1995).

In the present study we examine the effects of intense sound exposure on the chick ear at the level of the cochlear nerve. We report changes in neuron activity that exhibit both frequency-dependent and frequency-independent behavior. Moreover, most of the changes in activity immediately after removal from the exposure recovered within 12 days. This recovery occurs in an ear that retains a major structural defect in the partially regenerated tectorial membrane. Despite the recovery of most neuron activity, the coding of stimulus intensity for cells with characteristic frequencies (CFs) between 0.8 and 1.0 kHz continued to show abnormal behavior at 12 days. These unusual rate-intensity functions may be related to various factors including the tectorial membrane defect and/or abnormal function in the short hair cell system of the chick cochlea.

METHODS

Subjects and groups

Chicks (*Gallus domesticus*) were obtained as 1-day-old hatchlings from a commercial breeder (Truslow Farms, Cumberland, MD). When the animals were between 24 and 36 h old (1 day old) they were divided into exposed and control groups. The exposed chicks were placed individually in a wire mesh compartment suspended below a 30-cm speaker located in a sound-attenuated chamber. Six chicks at a time were exposed to an 0.9-kHz tone at 120 dB for 48 h. The second and third harmonics in this signal were 45 dB below the fundamental. The intensity of the stimulus was calibrated in the open field with a 12.5-mm condenser microphone (Brüel and Kjaer, Model 4125) and expressed as dB SPL relative to 20 μPa. Variability in the sound field was about $\pm$1.0 dB.

The exposed animals were further divided into a 0-day and a 12-day recovery group. Chicks in the 0-day recovery group were removed at the end of the 48-h exposure and immediately prepared for cochlear nerve testing. Given that it took ~1 h of preparation before the first cell was impaled and that testing might continue for a maximum of 6–7 h, the cells in the 0-day recovery group represented responses measured over a 1- to 7-h postexposure interval, and some degree of recovery will take place during this time. The accuracy in specifying the 12-day recovery groups varied between $\pm$18 h. The age-matched control animals were tested at 3 or 15 days of age, and these two age groups are referred to as 0-day or 12-day control animals to keep the nomenclature consistent.

Surgical preparation

Each animal was anesthetized with an intramuscular injection of a 25% solution of ethyl carbamate (urethane) at a dose of ~0.1 ml per day of age. When the animal was anesthetized, a tracheotomy was performed to maintain free breathing. The left ear canal was excised to expose the tympanic membrane. The tissue over the calvarium was removed, and the dissection was expanded to reveal much of the posterior-lateral skull surface. The skull was cleaned, and a thin layer of cyanoacrylate glue was applied to the ventral surface and allowed to dry. The chick was mounted in a head holder, and dental cement was applied to this region and the securing bracket of the holder. A hole ~5 mm diam was made through the left posterior-lateral portion of the skull above the temporal bone. This hole in the outer skull revealed the air-filled sinuses below. A 1.0- to 1.5-mm-diam hole was opened in the inner bony layer to reveal the endothelial lining of the lateral cochlear wall at the recussus tympani (Schwartzkopff and Bremond 1963). The lining was then gently pierced with a microdissecting pin and carefully retracted to the limits of the hole. With 1.0-mm holes, there was little if any perylimphatic fluid loss. Viewing through this fistula into scala tympani revealed a "whitish" band on the far or medial cochlear wall. This wall formed the cochlear limit of the superior fibrocartilagenous plate, and the cells of the cochlear nerve lay beneath its surface. Body temperature was maintained at 41°C with the use of a rectal probe and heating pad.

Acoustic calibration and recordings

A programmable frequency synthesizer (Audio Precision, Model "System One") was used to generate 1,767 discrete tone bursts (rise/decay time 5 ms, plateau 30 ms). These tone bursts covered the range of auditory space from 0.1 to 4.5 kHz (in 57 equally spaced logarithmic frequencies), with intensities from 0 to 100 dB SPL (in 31 intensity steps spaced 3.33 dB apart). A random sequence of these 1,767 stimuli was presented once during a test run, and the same sequence was used with every cell. The tone bursts were presented at a rate of nine per second, and it took 3.3 min to complete the series. A burst of band-limited noise (0.1–5.0 kHz) served as a search stimulus, and in control animals or 12-day recovered chicks, it was presented at a level of 80 dB SPL. In the 0-day recovered animals the noise burst was set to 100 dB SPL.

Stimuli were presented through a Beyer Dynamic DT-48 earphone. A sound tube (6.25 mm diam and 63 mm long) was sealed to the orifice of the earphone. A fitting at the end of the tube allowed an 0.5-mm probe-tube microphone (Entymotic, Model ER-7) to be positioned in the center of this tube. The probe tube extended 3.0 mm beyond the end of the sound tube, and when this assembly was sealed against the ear canal, the probe tube came to lie ~2.0 mm from the tympanic membrane surface. The electrical output of the probe microphone was connected to the signal analyzer side of System One. The second harmonic of the earphone and closed-tube sound delivery system was ~70–74 dB below the fundamental at frequencies >0.7 kHz, and 60–65 dB at frequencies <0.7 kHz. An automated calibration routine adjusted the voltage output of the synthesizer at the 57 test frequencies to achieve a constant stimulus of 100 dB SPL at the tympanic membrane. The stimuli were linear with regard to decibels of attenuation over a measured range of 70 dB. "System One" was programmed to change the signal voltage to produce the various SPLs at each test frequency. The stimulus conditions were calibrated for each animal at the start of the experiment.

Borosilicate capillary glass was pulled to achieve an impedance between 15 and 20 MΩ when filled with 3 M KCl. The electrode was mounted on a remotely controlled microdriver and advanced in 1.0-μm steps. The electrode was coupled to a high-impedance amplifier with a gain of $\times$1,000 (bandwidth 0.1–3.0 kHz). The amplifier output was monitored on an oscilloscope and connected to a level detector (Schmidt trigger) that converted the neural discharge to a 0.1-ms square-wave pulse. The interval between nerve spikes was measured by a double-buffered transient register (Modular Instruments, model M160 with a resolution of 0.1 ms). The register was triggered at the onset of each stimulus and spike counting was sampled over a 40-ms interval from stimulus onset. The buffer returned a spike count total to the computer, where it was stored in conjunction with the stimulus frequency and intensity. The spike analysis produced what is called a "spectral response plot" (Evans and Nelson 1973; Kaltenbach and Saunders 1987). This plot was constructed by representing the number of neural discharges associated with each stimulus presentation as a vertical bar whose height was proportional to the number of spikes.

This bar was appropriately positioned on a computer display in which the ordinate represented dB SPL and the abscissa was log frequency.

In ~10% of the animals tested, the exposed end of a Teflon-insulated silver wire (0.1 mm diam) was inserted through the hole in the cochlea. Compound action potentials detected by this electrode to a standard stimulus (a 1.0-kHz tone burst at 80 dB SPL) were periodically checked throughout the experiment to verify preparation stability. In the animals sampled, the response remained constant until the animal expired or the experiment was terminated.

Procedure

Each chick was anesthetized, surgically prepared, and tested in a double-walled acoustically shielded chamber. The sound tube was sealed over the ear canal and the stimuli were calibrated. The microelectrode was inserted into scala tympani, and then remotely advanced as the ear was stimulated with the search stimulus. Each cell was uniquely isolated, and extracellular responses typically had peak-to-peak levels between 0.4 and 1.5 mV. Once a cell was encountered, it was observed for 1–2 min to assure stable behavior. The spontaneous discharge was then sampled for 6.0 s in the absence of stimulation. The number of spikes sampled was converted to a rate per second and stored in a data file. The spectral response plot program was initiated and occasionally the level detector had to be readjusted to assure the proper counting of spikes. The plot was then labeled with a cell code and the data were stored on hard disk. The electrode was then advanced and the process was repeated when another cell was encountered. At the end of a track, the electrode was retracted, reoriented, and driven into the nerve trunk again, and this could be repeated many times. Occasionally, the electrode would rupture a blood capillary on the surface or within the fibrocartilagenous plate, which would inadvertently ruin the preparation (Manley et al. 1991).

Analysis of the spectral response plot

The spectral response plot has advantages and disadvantages. The major advantage is that much of the information contained in the neuron's behavior to sound can be obtained in a single test run. The resulting plot reveals the tuning curve clearly, and by slicing through the plot vertically or horizontally, isofrequency or isointensity contours can be obtained. The principle disadvantage is associated with the fact that avian cochlear nerve fibers exhibit high rates of spontaneous activity (Manley et al. 1991; Salvi et al. 1992, 1994), and this often makes the plot quite noisy. We have improved the signal-to-noise ratio in two ways.

First, the raw data were subject to a smoothing algorithm that calculated a running average on each data point (from low to high frequency along each isointensity condition) with the use of a three-point window. The smoothing procedure did not intrinsically alter the results. The spectral response plot for individual cells was evaluated from the smoothed data. The CF was determined by identifying the frequency that showed the lowest SPL at which a sound-driven response could be identified. Sometimes, a "best-guess" estimate was used when the CF appeared to fall between the discrete stimulus conditions that defined the spectral plot. The SPL at CF was also noted, and this is referred to as the CF threshold. The frequency selectivity of the receptive field (the tuning curve) was then ascertained with the $Q_{10\ dB}$ metric. With the use of the CF as a reference point, the frequency limits on the high- and low-frequency side of the tuning curve were determined at a point 10 dB above the CF threshold. The bandwidth at this 10-dB reference was determined, and the CF was then divided by the bandwidth to obtain the Q. The higher the value of Q, the sharper or more frequency selective was the receptive field of the cell. The spectral response plot was then sliced vertically at the CF to produce an isofrequency contour, more commonly called a rate-intensity function. Horizontal slices through the spectral response plot at 100, 80, 60, and 40 dB SPL yielded isointensity contours or frequency response–area functions (Rose et al. 1971).

The second procedure for improving the signal-to-noise ratio synthesized the results from a number of cells by averaging the raw discharge counts at each frequency-intensity combination within the spectral response plot. This is a rather unorthodox procedure, but well-defined criteria were used in selecting cells for these averages. The averaged tuning curve was constructed by choosing individual spectral response plots from cells within a narrowly defined range of CFs and CF thresholds. The window about each of these variables was typically less than ±75 Hz and ±2 dB. When an averaged rate-intensity function was plotted, the frequency window might be wider, but the CF thresholds were kept to ±2 dB. Generally, all the cells lying within the defined window were used in the averaged function, but if the number became excessively large, the sample was reduced to a maximum of 10 or 11 cells by random selection. The averaged data (derived from the raw spike counts) was then subjected to the smoothing routine described above. These averaged spectral plots were, of course, derived from cells within the same group.

RESULTS

Data were obtained from 903 cells (268 in 0-day controls, 223 in 12-day controls, 213 in 0-day recovered animals, and 199 in 12-day recovered animals). A total of 82 animals were tested, with an average return of ~11 cells per animal. In >50% of the chicks, between 18 and 37 cells were logged. Testing never exceeded 6.5 h (from anesthetization) and averaged 4.75 h over all chicks. There were no identifiable testing differences between the two age groups; however, the older animals (15 days old) were obviously larger and appropriate changes in head and electrode orientation were required.

Control cells

The cochlear nerve responses were essentially the same in the 0-day and 12-day control chicks in terms of CF threshold, $Q_{10\ dB}$, and spontaneous rate. Figure 1 plots the CF threshold for control cells in the two age groups, and the appearance of the scatter plots on the *left* and *right* is very similar. However, there was an absence of cells at <0.2 kHz in the older chicks (*right*) because the electrode could no longer be oriented toward the extreme apical region of the nerve (Manley et al. 1991).

The frequency region from 0.2 to 4.5 kHz was divided into seven equal intervals (on the logarithmic frequency axis), and CF thresholds for all control cells within each interval were averaged. The average threshold value (Fig. 1, filled circles) was placed at the center frequency for each interval and the resulting plots in the two panels provided a summary of the CF thresholds for each age group. The data contained in these seven intervals, for the two control groups, were analyzed with a two-way analysis of variance for age and frequency. This analysis revealed a significant frequency effect (as expected by the U-shaped curves) ($F = 62.3$, df = 6,462; $P < 0.01$), but no difference by age ($F = 0.6$; df = 1,462; $P > 0.05$). Thus the scatter of data in each group was due to chance sampling. Interaction between age and frequency was also insignificant ($F = 1.87$; df = 6,462; $P > 0.05$).

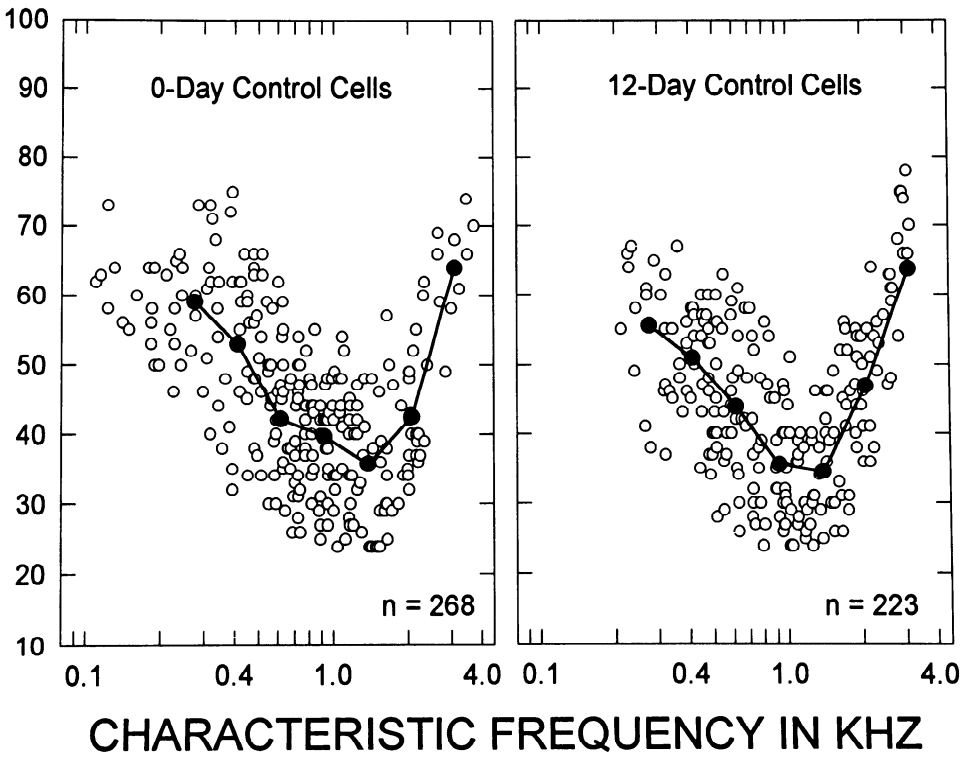

FIG. 1. Characteristic frequency (CF) thresholds are plotted for the 0-day (*left*) and 12-day (*right*) control cells. Filled circles: average CF thresholds for cells contained in the respective logarithmic intervals.

The results in Fig. 2 illustrate the values of $Q_{10\,dB}$ (*A* and *B*), and spontaneous activity (*C* and *D*), plotted against the CF of cells examined in the 0-day and 12-day control chicks. The $Q_{10\,dB}$ values in both age groups showed that frequency selectivity increased above 0.2 kHz in an orderly way. Regression lines were fit to the data above 0.2 kHz, and their slopes were similar (7.81 for the 0-day and 7.34 for the 12-day control cells).

Figure 2, *C* and *D*, show spontaneous activity, and these data ranged from 8 spikes/s to near 100 spikes/s. Regression lines fit to both age groups showed only a slight downward tilt toward the high frequencies, indicating that the level of this activity was largely independent of frequency. The average spontaneous activity in the younger chicks was slightly lower than in the older animals (mean for younger chicks: 25.0 spikes/s; mean for older chicks: 27.0 spikes/s), but this 2-spike difference, when examined with an independent samples *t*-test, was due to chance sampling (t = 1.71, df = 489, $P > 0.05$).

The results in Figs. 1 and 2 indicate that CF threshold, $Q_{10\,dB}$, and spontaneous activity were the same in both control groups. Thus we feel justified in combining these data into a single control condition for some of the comparisons that follow.

Two averaged spectral response plots appear in Fig. 3, *A* and *C*. These plots were constructed from a sample of 0-day control cells that were within ±5% of the mean CFs indicated on the figure. The two CFs were selected somewhat arbitrarily, but with the provision that they were well separated from each other. The CF threshold levels, however, were within 5 dB of the lowest CF thresholds seen in Fig. 1, *left* (for the respective frequencies). Figure 3*A* is the average of all the cells meeting this frequency and threshold criteria; they had a mean CF and CF threshold of 0.57 kHz ± 10.9 (SE) Hz and 32 ± 0.84 (SE) dB. Figure 3*B* shows response-area functions (in 20-dB steps) for the spectral plot in Fig. 3*A*. The low-frequency slopes of the four contours at 100, 80, 60, and 40 dB, were 0.25, 0.26, 0.27, and 0.32 spikes/Hz, whereas on the high-frequency side they were somewhat steeper, but also similar to each other (0.67, 0.54, 0.48, and 0.52, spikes/Hz, respectively).

A second tuning curve (derived from 6 cells) is presented in Fig. 3*C*. The average CF and CF threshold was 1.53 kHz ± 11.2 (SE) Hz and 28 dB SPL ± 1.06 (SE) dB. The response-area functions for this tuning curve appear in Fig. 3*D*, and the contours plotted at 100, 80, 60, and 40 dB were nearly symmetrical on both the high- and low-frequency side. The slopes on the low-frequency side of the contours were 0.15, 0.19, 0.21, and 0.17 spikes/Hz, respectively, whereas on the high-frequency side they were 0.19, 0.23, 0.24, and 0.16 spikes/Hz. Finally, the $Q_{10\,dB}$ value for this tuning curve was 7.38, whereas in Fig. 3*A* it was only 3.61. The averaged values of $Q_{10\,dB}$ derived from the Q values of individual cells in these samples were 7.27 and 3.52, respectively, and this was very similar to the $Q_{10\,dB}$ obtained from the averaged spectral response plot. The close correspondence between these two measures of Q provided a measure of validation for the averaging procedure.

Figure 4 offers three pairs of spectral response plots obtained from single cells with the data smoothed by the three-point running average. Cells in *A* and *B*, *C* and *D*, and *E* and *F* had the same approximate CF and CF threshold. The interesting aspect of these tuning curves was the fact that their sharpness of tuning was very different. The values of $Q_{10\,dB}$ for *A*, *C*, and *E* were 4.15, 3.87, and 4.29, whereas for *B*, *D*, and *F* they were 6.95, 7.98, and 8.15, respectively. These examples are representative of many cases in which cells with a common CF and CF threshold had dramatically different levels of frequency selectivity.

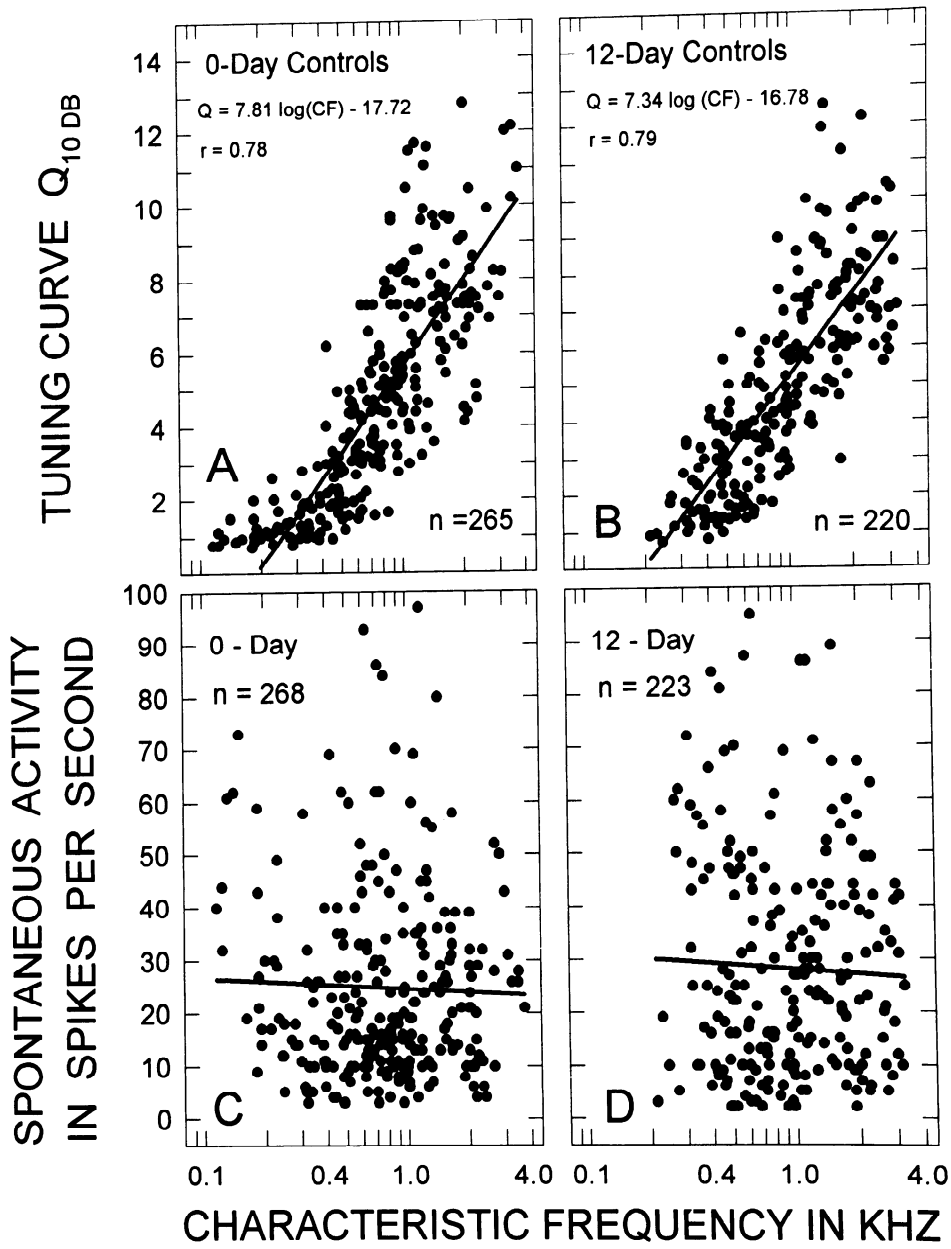

FIG. 2. Values of $Q_{10\ dB}$ and spontaneous activity are plotted at each cell's CF for the 0-day and 12-day control groups. Solid lines: best-fit regression lines to the data.

This aspect of the data is further considered in Fig. 5. The CF thresholds from control cells in both age groups were subdivided into two compartments. Figure 5*A* represents a group of cells with the most sensitive CF thresholds. Sensitivity was defined as all those cells within 5–8 dB of the "best" CF thresholds in the 0-day and 12-day control groups. A second sample of cells (Fig. 5*C*) was identified with CF thresholds within 5–8 dB of the "poorest" thresholds. This parceling of the control cells produced two discrete samples of CF thresholds completely independent of each other. The threshold average between 1.2 and 1.5 kHz, for example, was 27.5 dB (Fig. 5*A*) and 45.0 dB (Fig. 5*B*).

The $Q_{10\ dB}$ for these two sets of cells are plotted in Fig. 5, *B* and *D*. The frequency axes of these plots were divided into equal (logarithmic) intervals and the average and standard deviation of the Q value for the cells in each interval were calculated. The gray dots and standard deviation (vertical) bars show the result of this analysis. The variability in $Q_{10\ dB}$ was greatest between 0.8 and 2.0 kHz for both groups of cells, and frequency selectivity for the better threshold cells was sharper (had larger Q values) than for the poorer threshold cells. A two-way analysis of variance on the five overlapping points between 0.37 and 3.3 kHz in Fig. 5, *B* and *D*, showed a significant difference in $Q_{10\ dB}$ between groups (F = 34.4; df = 1, 255; $P < 0.01$). As might be expected, a significant frequency effect was noted (F = 95.7; df = 4, 255; $P < 0.01$). The interaction between Q and frequency was also significant (F= 2.77; df = 4,255; $P < 0.05$). This analysis indicated that $Q_{10\ dB}$ depended on the CF threshold of the cell.

A comparison between rate-intensity functions in cells with better or poorer CF thresholds, using the data identified in Fig. 5, *A* and *C*, was undertaken to determine whether sensitivity had any influence on the coding of stimulus intensity. Figure 6*A* shows rate-intensity functions for groups of cells over the indicated frequency range. The cells in each

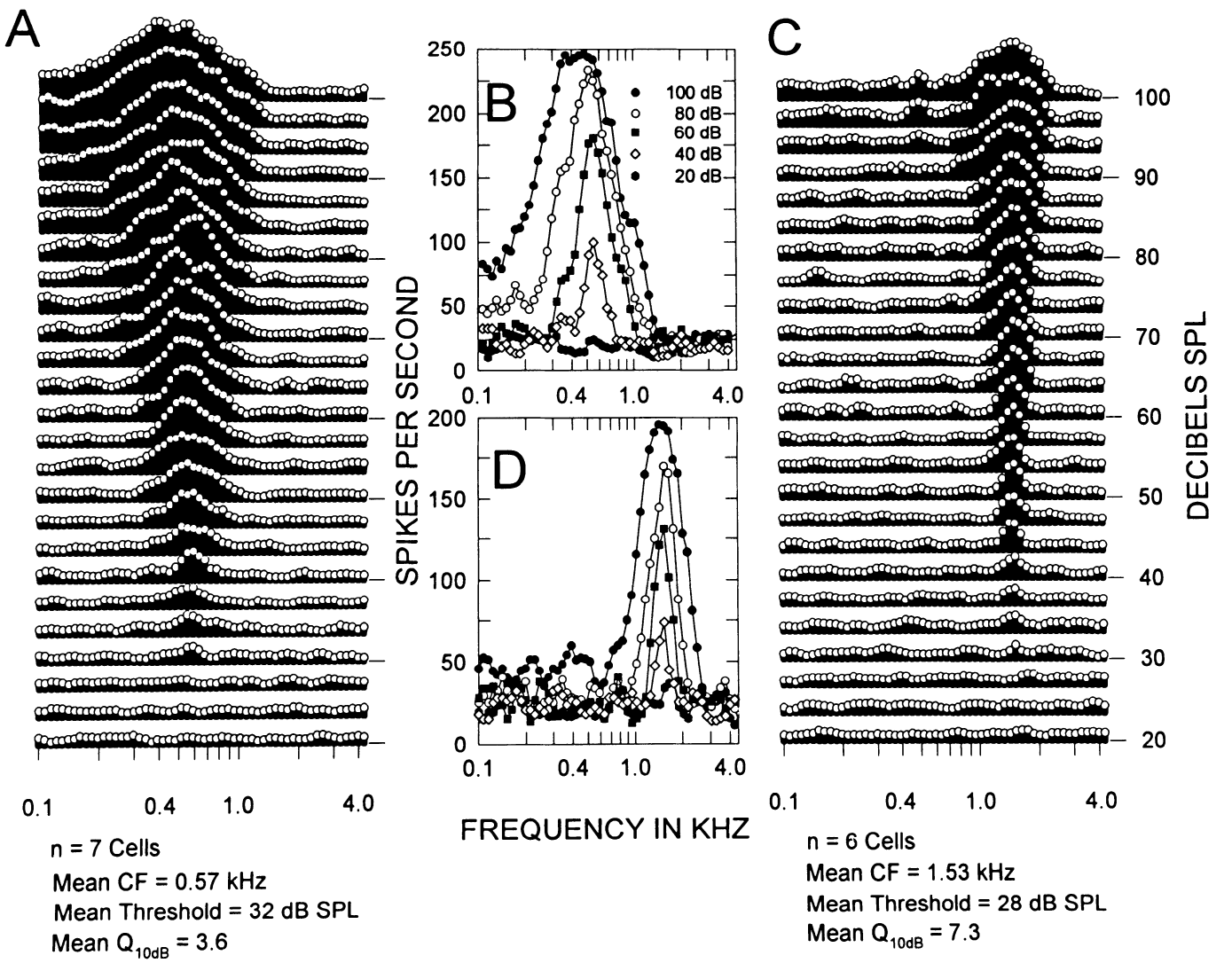

FIG. 3. *A* and *C*: examples of averaged tuning curves in 0-day control cells. *B* and *D*: response-area functions for the respective tuning curves. The shape of the tuning curve in both these examples remained fairly symmetrical about the CF at all stimulus levels.

plot were nearly equally divided between the 0-day or 12-day control animals to eliminate any age effect. The frequency of the sample in each plot varied over the indicated range, whereas the CF thresholds had a more restricted range that was ±1.6 dB at most. Three additional frequency ranges were plotted (results not presented) for cells with CFs in the 0.1- to 0.18-kHz, 0.19- to 0.34-kHz, and 2.08- to 3.81-kHz ranges. Several interesting things emerge. First, the shift to the right in the rate-intensity function of the poorest cells represents the difference in CF threshold sensitivity. Second, the cells in both samples showed response saturation at a level of ~200 spikes/s. The slopes of the rate-intensity functions in the best-CF-threshold group, over all six frequency ranges analyzed, averaged 4.30 ± 0.25 (SE) spikes $\cdot s^{-1} \cdot dB^{-1}$. It was 4.95 ± 0.20 (SE) spikes $\cdot s^{-1} \cdot dB^{-1}$ for the poor-CF-threshold group. A *t*-test for independent samples revealed that the slopes in these two groups were due to chance sampling (t = -2.11, df = 10, $P > 0.05$). It thus appears that the coding of stimulus intensity was independent of CF threshold.

Figure 6*B* compares rate-intensity functions in 0-day and 12-day control cells over the indicated range of frequencies. The analysis was also expanded to include three additional frequency ranges, as noted above (results not reported). The cells sampled within each rate-intensity plot all had the same approximate CF threshold (maximum range ±1.4 dB). The important point to be gleaned from Fig. 6*B* is that the coding of stimulus intensity was different at the two ages. Over all frequencies, older chicks had a steeper growth rate (5.73 spikes $\cdot s^{-1} \cdot dB^{-1}$), and a higher plateau of driven activity (259 spikes/s), than observed in the younger animals (3.62 spikes $\cdot s^{-1} \cdot dB^{-1}$ and 201 spikes/s, respectively). In addition, the dynamic range (i.e., the dB change from threshold to saturation) averaged 49.6 dB in the 0-day controls but was only 39.9 dB in the older animals. Thus there was an 8.8-dB compression in the rate-intensity functions from 3 to 15 days of age. This age difference was first reported by Manley et al. (1991), and the results above suggest that it occurs at all frequencies. The compressive dynamic range is interesting because it is opposite that reported in the kitten (Dolan et al. 1985; Kettner et al. 1985; Romand 1984; Walsh and McGee 1987). Older kittens showed a larger dynamic

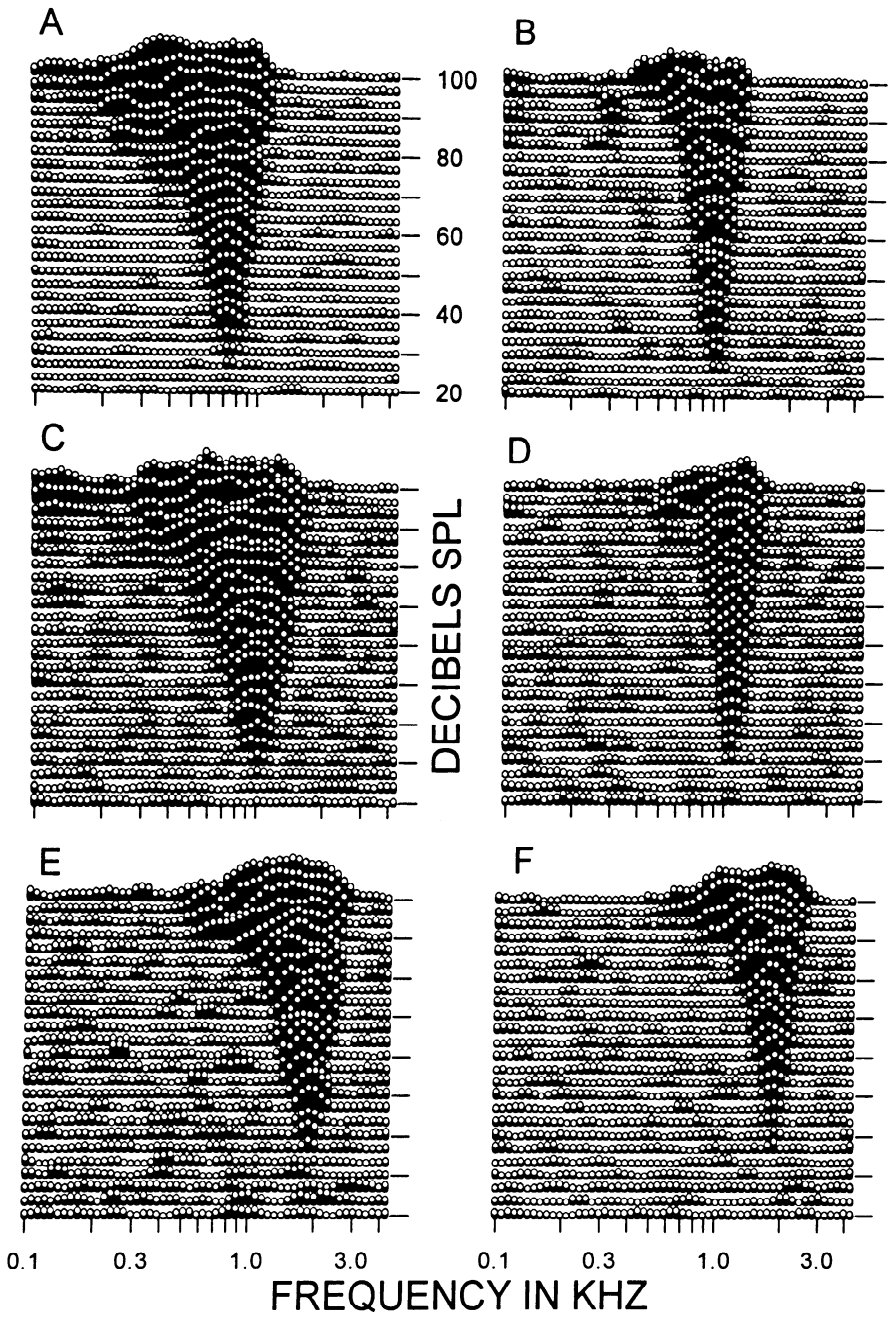

FIG. 4. Six examples of tuning curves are presented for individual control cells. Each of these curves has been smoothed (see text). Cells in *A* and *B*, *C* and *D*, and *E* and *F* have the same approximate CF and CF threshold. However, the $Q_{10\,dB}$ in *A*, *C*, and *E* is substantially smaller than that in *B*, *D*, and *F*.

range than younger animals. The mechanism of this species difference remains to be identified.

The relation between spontaneous activity and CF sensitivity is considered in Fig. 7. All control cells were organized into three groupings on the basis of arbitrarily chosen ranges of spontaneous activity (0–12, 20–32, and 40–52 spikes/s). The solid lines show the running averages (with the use of a window of 9 adjacent data points) for the low-spontaneous-activity cells (0–12 spikes/s) and the highly active cells (40–52 spikes/s). Below 1.0 kHz the low-spontaneous cells had the poorest CF thresholds, whereas the highly active cells exhibited better threshold sensitivity. Above 1.0 kHz this relationship becomes less clear as the running average lines converge.

Finally, it is important to consider the stability of CF thresholds within a test session. Figure 8, *left,* describes the CF thresholds in two groups of control cells. The early group were the first three to five cells and the late group were the last three to five cells measured within a session. The estimated time over which the early cells were sampled was 38 min (after the 1st cell was encountered). The late cells were obtained between 175 and 223 min after the first cell. The results showed that the distribution of CF thresholds was the same despite the 3-h difference between the two groups. These data indicate that cochlear nerve activity was stable throughout testing.

Zero-day recovered cells

The preparation of 0-day recovered animals was identical to that of control animals, and the likelihood of recording

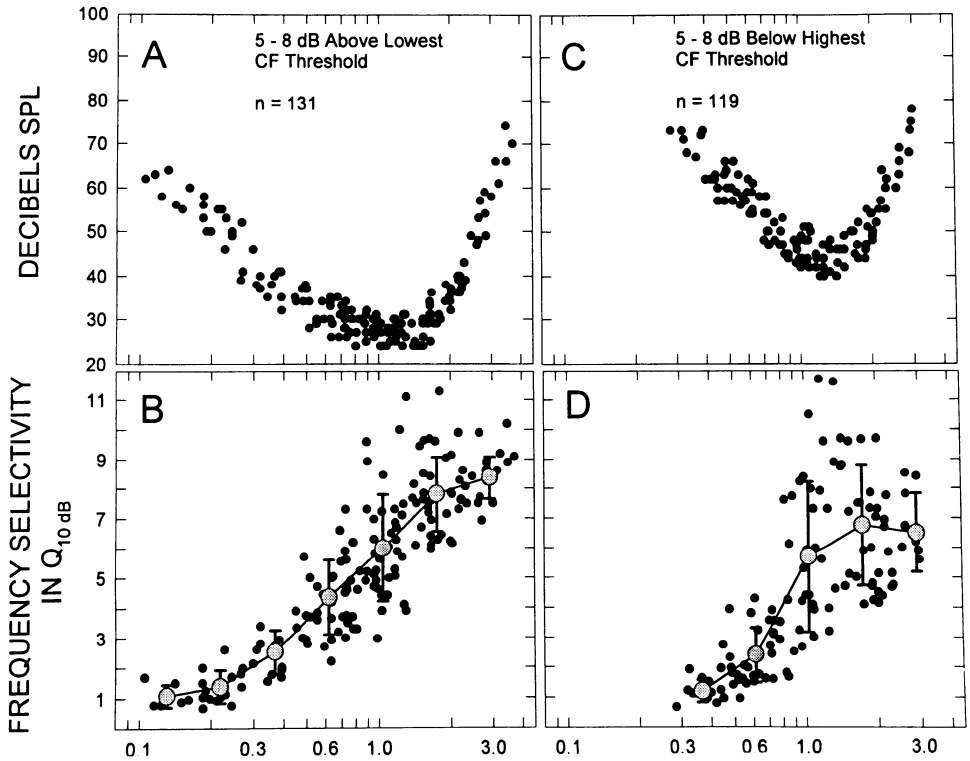

FIG. 5. *A* and *C*: best and poorest CF thresholds for the entire sample of control cells. There is a difference of ~17 dB in threshold between these 2 samples. *B* and *D*: values of $Q_{10\,dB}$ for these 2 samples. Large circles with vertical bars: average Q values and standard deviations for collections of cells in successive logarithmic intervals along the frequency axis. Note the increased variability and difference in average values for the best- and worst-CF-threshold cells.

from cells was also the same. The search stimuli, however, had to be made more intense in order to identify cells, and the overall identification was made more difficult because of a substantial reduction in spontaneous activity.

Figure 8, *right,* shows CF thresholds in 0-day recovered cells examined early or late within a test session. A difference of approximately 3 h also separated these two samples, and the fact that the two groups overlapped each other indicated stable measurement conditions. Some recovery of threshold might be expected during this 3-h interval, and it has been reported that threshold shift recovers at a rate of ~1 dB/h during the first 24 h postexposure (McFadden and Saunders 1989; Pugliano et al. 1993b). Thus 3 dB of recovery would be expected in the 3-h interval for the data in Fig. 8, *right.* The results in Fig. 8, *right,* extend over a 40-dB range, and a 3-dB change may be masked by the variance in CF thresholds.

A comparison between control and exposed CF thresholds is seen in Fig. 9. Between 1.1 and 1.3 kHz, the most sensitive control thresholds were at ~24 dB, whereas the least sensitive thresholds in the exposed cells were as high as 93 dB. This represents a maximum threshold shift of 69 dB. A comparison between the most sensitive control and exposed cells revealed a threshold shift of only 49 dB at these same frequencies. Figure 9 also shows that threshold shift was smallest in the lowest (0.1–0.3 kHz) and highest (2.7–3.5 kHz) CFs. Indeed, there was overlap in the exposed and control CF thresholds between 0.1 and 0.5 kHz. Nevertheless, the best control thresholds in this frequency range were better than the most sensitive thresholds in the exposed cells. At the highest frequencies, the control and exposed data also converged on each other, but the thresholds did not overlap.

Figure 10, *top,* illustrates the difference between 0-day control and 0-day recovered $Q_{10\,dB}$. The frequency selectivity for cells with CFs between 0.1 and 0.5 kHz showed the same $Q_{10\,dB}$ in both groups. The average $Q_{10\,dB}$ for the control cells within this frequency range was 1.78 ± 0.11 (SE), whereas in the 0-day recovered cells it was 1.82 ± 0.12 (SE). An independent samples t-test revealed that the mean difference between these groups was due to random sampling. The frequency selectivity of control and exposed cells increasingly diverged as the CF rose above 0.5 kHz. By way of example, the Q value for control cells between 1.0 and 2.0 kHz averaged 7.18 ± 0.28 (SE), but it was only 2.23 ± 0.15 (SE) in the 0-day recovered cells. The difference between these mean values was statistically reliable (t = 15.5, df = 117, $P < 0.01$). The solid lines in Fig. 10, *top,* represent the regression on the data (>0.5 kHz), and are only presented to emphasize differences between the groups. The conclusion from these data is that sound exposure caused a severe deterioration in frequency selectivity, but only at >0.5 kHz.

Figure 10, *bottom,* shows the changes in spontaneous activity. The control and exposed data were also fit with regression lines, both of which showed a slight downward tilt toward the high frequencies. The horizontal orientation of these lines indicated that the distribution of spontaneous activity was largely independent of frequency. Spontaneous activity in the 0-day recovered cells, however, was greatly suppressed and averaged only 9.7 ± 0.62 (SE) spikes/s. The highest discharge rate was 38 spikes/s, with many cells showing no spontaneous activity at all. The spontaneous activity in control cells, in contrast, averaged 25 ± 1.11 (SE) spikes/s, with a maximum of 98 spikes/s and minimum of 3 spikes/s. The difference in mean spontaneous activity between these conditions was statistically reliable (t = 9.48, df = 479, $P < 0.01$).

Examples of tuning curves, response-area functions, and

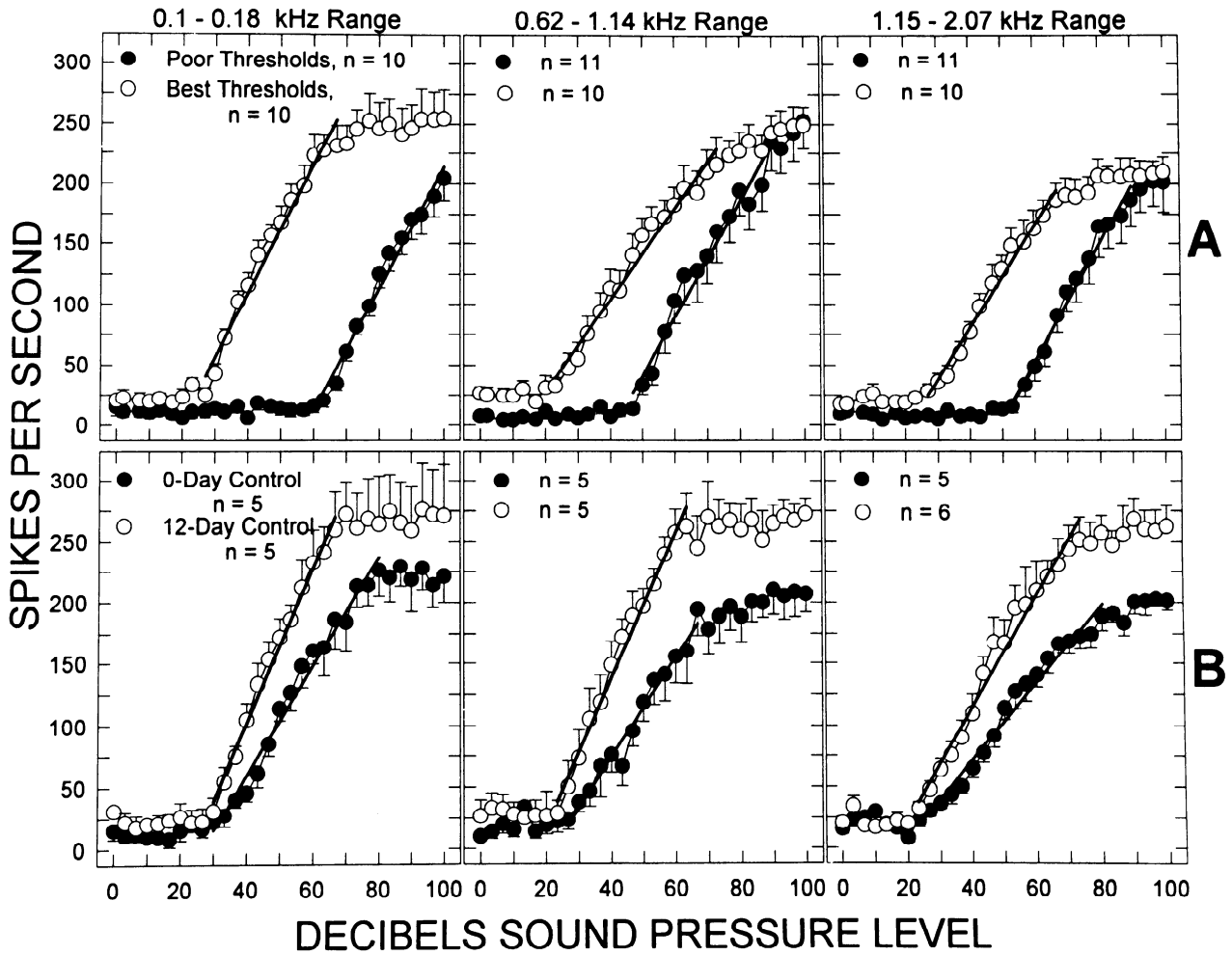

FIG. 6. Rate-intensity functions averaged from the indicated number of control cells over the respective frequency range. *A*: cells with the best and worst CF thresholds as defined in Fig. 5. About half the cells in each of these plots come from the 2 age groups. *B*: functions from samples of cells from the 2 ages. Plots have the same threshold, but the 12-day cells have a steeper growth curve and saturate at a higher spike level.

rate-intensity functions are given for 0-day exposed cells in Fig. 11. The tuning curves in Fig. 11, *A* and *B*, were averaged from six cells each, and the CF in Fig. 11*A* was 1.17 kHz, whereas in Fig. 11*B* it was 2.16 kHz. A severe loss in the sensitivity of the tip region cells was apparent. Figure 11, *C* and *D*, shows response-area functions for the respective tuning curves. The tuning curve appeared symmetrical on the high- and low-frequency sides, but had a pronounced loss of sensitivity in the tip region. Finally, Fig. 11, *E* and *F*, shows rate-intensity functions (at CF) for these tuning curves. Compared with the control rate-intensity functions (see Fig. 6*B*), the growth portions of these curves were shifted to the right. This, of course, is expected from the threshold shift in these cells. In addition, the spike growth rate was much steeper than in control cells, and the dynamic range from threshold to saturation was only ~20 dB.

Rate-intensity functions in samples of 0-day control and exposed cells appear in Fig. 12 for frequencies between 0.24 and 2.53 kHz. The average CF of the sample is given in each panel, and although the range of CFs could be as great as 10% of the mean, the CF thresholds were tightly controlled and had a range between 1 and 2 dB. The control and exposed cell thresholds in each frequency range were within 5 dB of the best CF thresholds for each group (see Fig. 9). The exposed cells showed a threshold shift relative to the control cells that was between 30 and 50 dB for the 0.88-, 1.44-, and 2.53-kHz functions. In addition, the growth rate of the exposed cells (between 8.8 and 2.53 kHz) was quite steep, being on the order of 9.1 spikes $\cdot s^{-1} \cdot dB^{-1}$. The control cells showed a much shallower growth of ~4.2 spikes $\cdot s^{-1} \cdot dB^{-1}$. The saturation level of the control and exposed cells were about the same. The dynamic range of the control functions averaged 45.6 dB, whereas in the exposed cells it was only 18.3 dB. The results for control and exposed cells with CFs at 0.24 and 0.28 kHz are consistent with the small threshold shift seen at these frequencies (see Fig. 9).

Twelve-day recovered cells

All the birds assigned to the 12-day recovered group survived, and the ability to encounter cells was identical to that in control animals. Figure 13 compares CF thresholds in 12-day control and 12-day recovered cells. The two sets of data overlap each other, and it was obvious that the CF thresholds recovered completely.

The same conclusion can be made for ($Q_{10\,dB}$) and spontaneous activity (Fig. 14, *top* and *bottom*). The results in Fig.

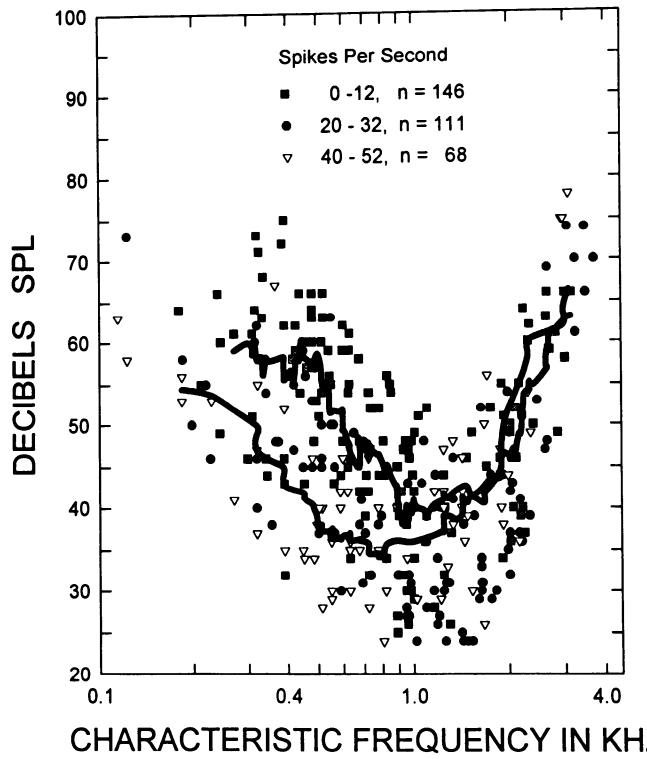

FIG. 7. All the control cells shown here are differentiated by spontaneous activity. Solid lines: running averages for the groups of cells with the lowest (0–12 spikes/s) and highest (40–52 spikes/s) spontaneous rates. Below ~1.0 kHz the cells with higher spontaneous activity have better CF thresholds. Above 1.0 kHz spontaneous rate does not appear related to CF threshold.

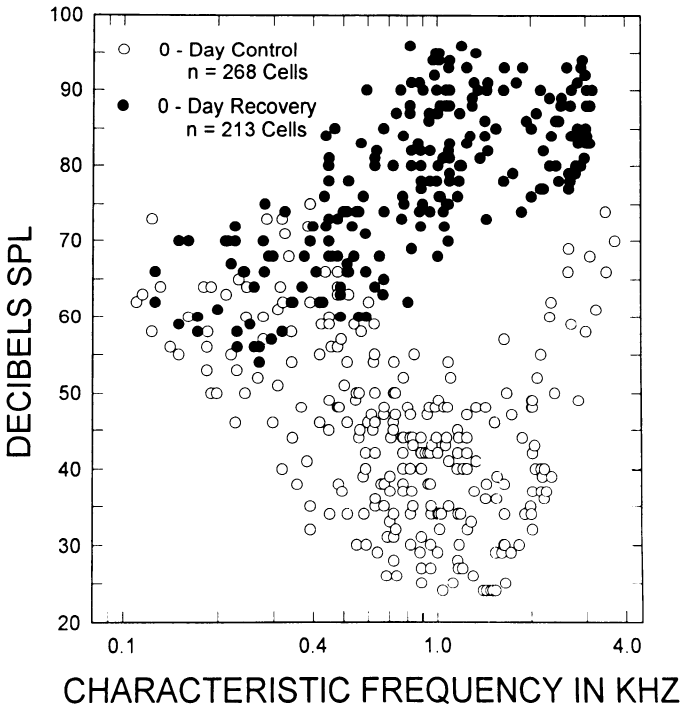

FIG. 9. CF thresholds for the 0-day control and the 0-day recovered cells. The effect of intense sound on CF threshold is apparent.

14, *top,* show that tuning curve sharpness returned to normal, as shown by the regression lines and correlation coefficients (r), which were nearly the same. Similarly, regression lines for spontaneous activity in Fig. 14, *bottom,* were nearly identical to each other. The horizontal orientation of the regression lines further indicated that spontaneous activity was independent of frequency. The averaged spontaneous activity in the control and exposed cells was 28.2 and 28.7 spikes/s, respectively, and this difference was due to chance sampling ($t = 0.24$, df = 422, $P > 0.05$).

Figure 15 shows a rate-intensity function for samples of 12-day recovered and control cells. The range of CFs was less than ±40 Hz for each sample, and CF thresholds were within ±2.8 dB of each other. The cells chosen at each frequency were within 5 dB of the lowest CF thresholds found in Fig. 13. The 12-day recovered cells had about the same spontaneous activity and CF threshold levels as the

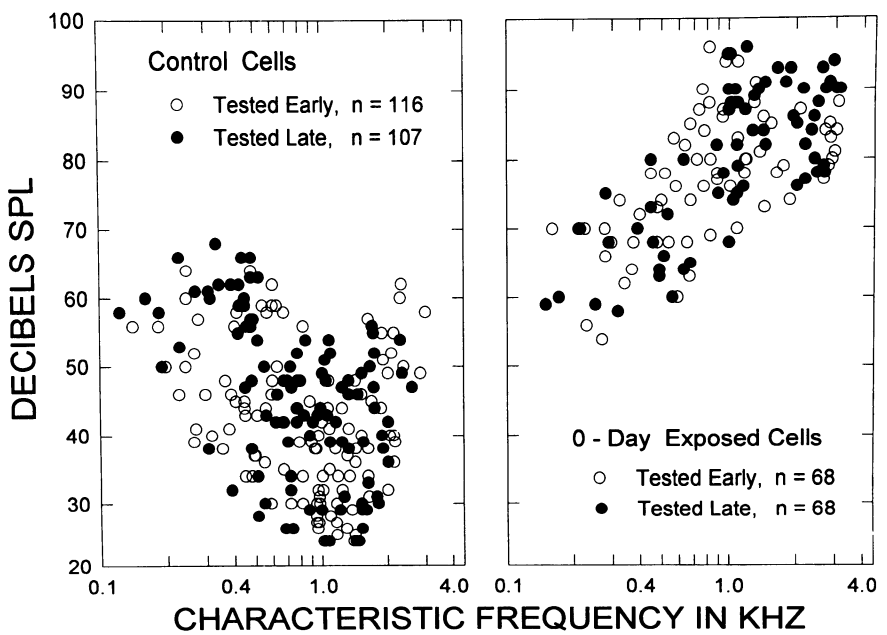

FIG. 8. Comparison of CF thresholds in groups of cells whose results were obtained either early or late in the test session. These groups are separated by ~3 h, and as can be seen, the CF threshold data overlap each other. *Left*: control cells. *Right*: 0-day recovered cells. Both *left* and *right* indicate that the duration of the experiment did not influence CF threshold.

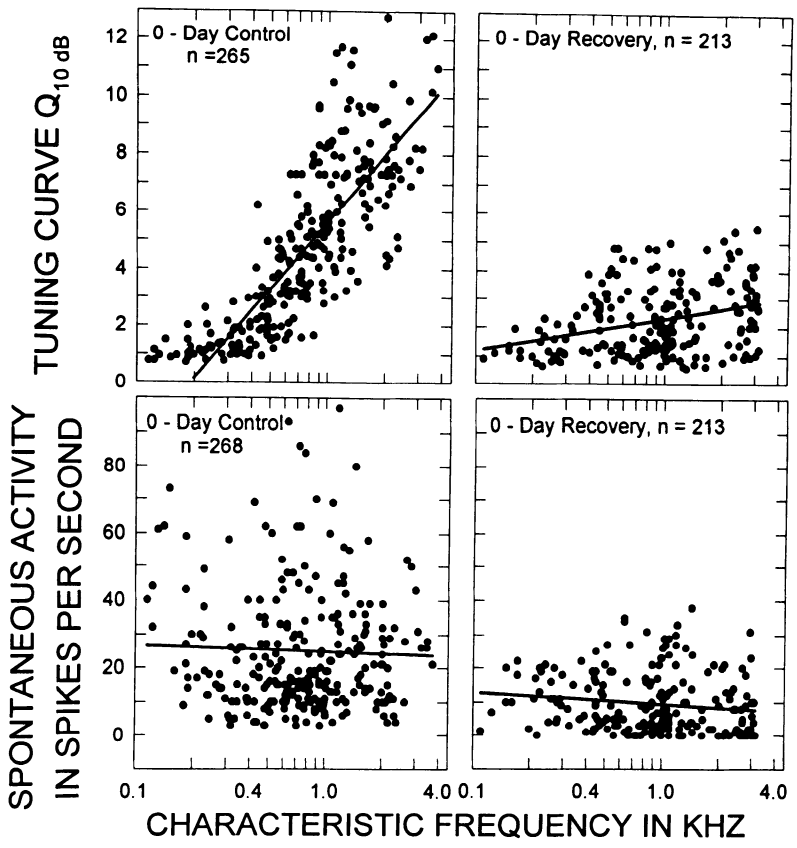

FIG. 10. *Top*: values of $Q_{10\ dB}$ for 0-day control and exposed cells. Solid lines: fit to the data. *Bottom*: spontaneous activity for the control and exposed groups. Regression lines are also fit to these data.

controls. The most startling observation, however, was the abnormally high spike growth rate and excessive response level at saturation for recovered cells with CFs at 0.81 and 1.02 kHz. A hint of excessive response rate was seen at 0.4 kHz, whereas the rate-intensity functions at 1.42 and 2.0 kHz were the same for both groups. These abnormal rate-intensity functions may represent a long-lasting consequence of acoustic injury to the chick ear.

DISCUSSION

Control cells

Discharge patterns for cochlear nerve cells have been reported in a number of avian species including adult and young chickens (Manley et al. 1991; Salvi et al. 1992, 1994). The results reported here for control animals were, for the most part, similar to these earlier data, and to observations from the nucleus magnocellularis (Cohen and Saunders 1993; Warchol and Dallos 1990). Nevertheless, the current CF thresholds were 10–15 dB poorer than those in adults (Salvi et al. 1992, 1994), but nearly identical to those reported for younger animals (Manley et al. 1991). These age effects may be due to middle-ear maturation rather than intrinsic changes in the cochlea or cochlear nerve. The chick skull continues to expand for >70 days posthatching and is accompanied by a steady increase in the size of all middle-ear components (Cohen et al. 1992a). In addition, admittance magnitude or velocity transfer functions, measured at the tympanic membrane, reveal functional improvements in sound conduction over a similar time interval (Cohen et al. 1992b; Saunders et al. 1986). Improvements in middle-ear function over the 12-day interval between the two control groups used here would be expected to cause a 2- to 4-dB improvement in sensitivity, and this is much less than the variability in CF thresholds (Fig. 1).

The fact that our control cells replicated the observations of others, that there were no age differences (with exception of the rate-intensity functions), and that the responses were stable over time (see Fig. 8), leads to the conclusion that the neuron activity reported here was a valid indication of cochlear nerve behavior.

Effects of intense sound exposure

The consequences of overstimulation in the 0-day recovered chicks were pronounced, and all aspects of cochlear nerve activity showed a loss in function. Moreover, the magnitude of functional recovery in the cochlear nerve at 12 days of recovery was as remarkable as the degree of impairment at 0 days. These observations parallel previously reported results for evoked potential or single-cell activity recorded from the nucleus magnocellularis of sound-exposed chicks (Adler et al. 1992, 1993; Cohen and Saunders 1993; McFadden and Saunders 1989; Pugliano et al. 1993a,b; Saunders et al. 1993).

The most important question posed by these observations is whether or not they tell us anything about the mechanisms that lead to the loss and recovery of function. To identify potential mechanisms, it is necessary to consider the organization of the avian basilar papilla and the changes in that organization caused by overstimulation. The papilla contains tall and short hair cells (Smith 1985; Takasaka and Smith

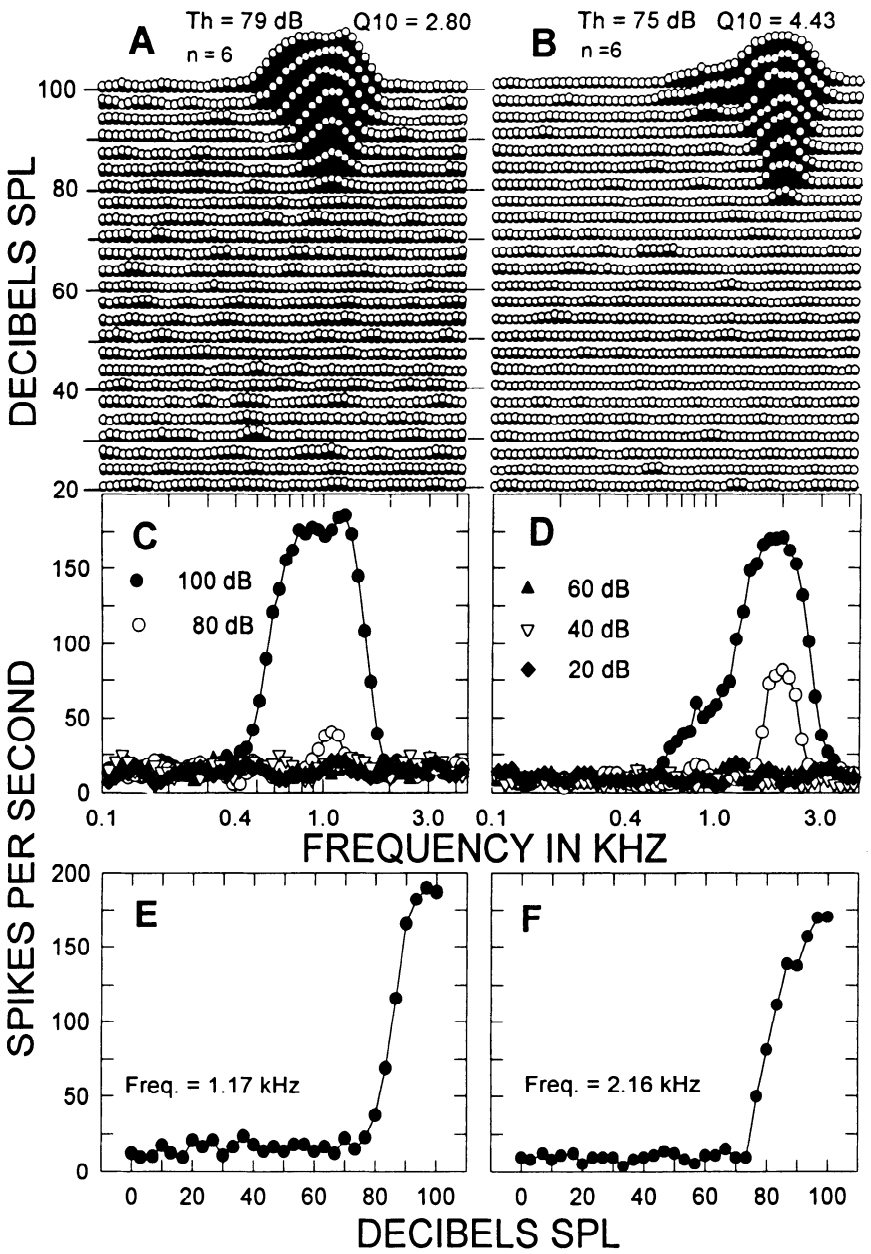

FIG. 11. *A* and *B*: 2 examples of averaged 0-day recovered tuning curves. The loss of sensitivity in the tip region of the receptive field is obvious. *C* and *D* and *E* and *F*: response area curves and the rate-intensity functions (at the CF) for the 2 tuning curves.

1971; Tanaka and Smith 1978) differentiated by the lengths of their cell bodies, their patterns of innervation, and their locations on the papilla surface. The short hair cells are found above the basilar membrane on the "mobile," "inferior," or "abneural" side of the papilla. The tall hair cells are located on the "immobile," "superior," or "neural" portion of the papilla above the superior fibrocartilagenous plate (see drawing in Fig. 16*A*). Afferent fibers dominate tall hair cell innervation, whereas efferent fibers dominate the innervation of short hair cells. Transitional or so-called "intermediate" hair cells, innervated by approximately one afferent and one efferent neuron (Fisher 1992, 1994), are found along the limbic border at the junction between the fibrocartilagenous plate and basilar membrane (Takasaka and Smith 1971).

The patch lesion destroys primarily short hair cells, although Cotanche (1987a) suggested that the superior or neural edge of this lesion may encroach on the tall hair cell field. Research from our laboratory, with the use of the 0.9-kHz exposure, indicated that the patch and stripe lesions extended minimally beyond the limbic border (Saunders, unpublished observations). Although some of the transitional cells were destroyed by the exposure, it appears that the tall hair cell field remained largely intact (Henry et al. 1988; Marsh et al. 1990). Indeed, the recent review by Cotanche et al. (1994) noted that tall hair cells were "rarely lost" at exposure levels <125 dB. This observation may be peculiar to the young chicken, because acoustic injury in the adult quail appeared to spread into the tall hair cells (Ryals et al. 1989).

The earliest postexposure appearance of new hair cells is between 90 and 100 h after the onset of the exposure (Cotanche 1987a; Raphael 1992, 1993; Stone and Cotanche 1992). With the exposure used here we see emergent hair cells between 2 and 3 days postexposure (Saunders, unpublished observations), with a substantial increase in new hair cells on the 4th day (Marsh et al. 1990). It may take these new

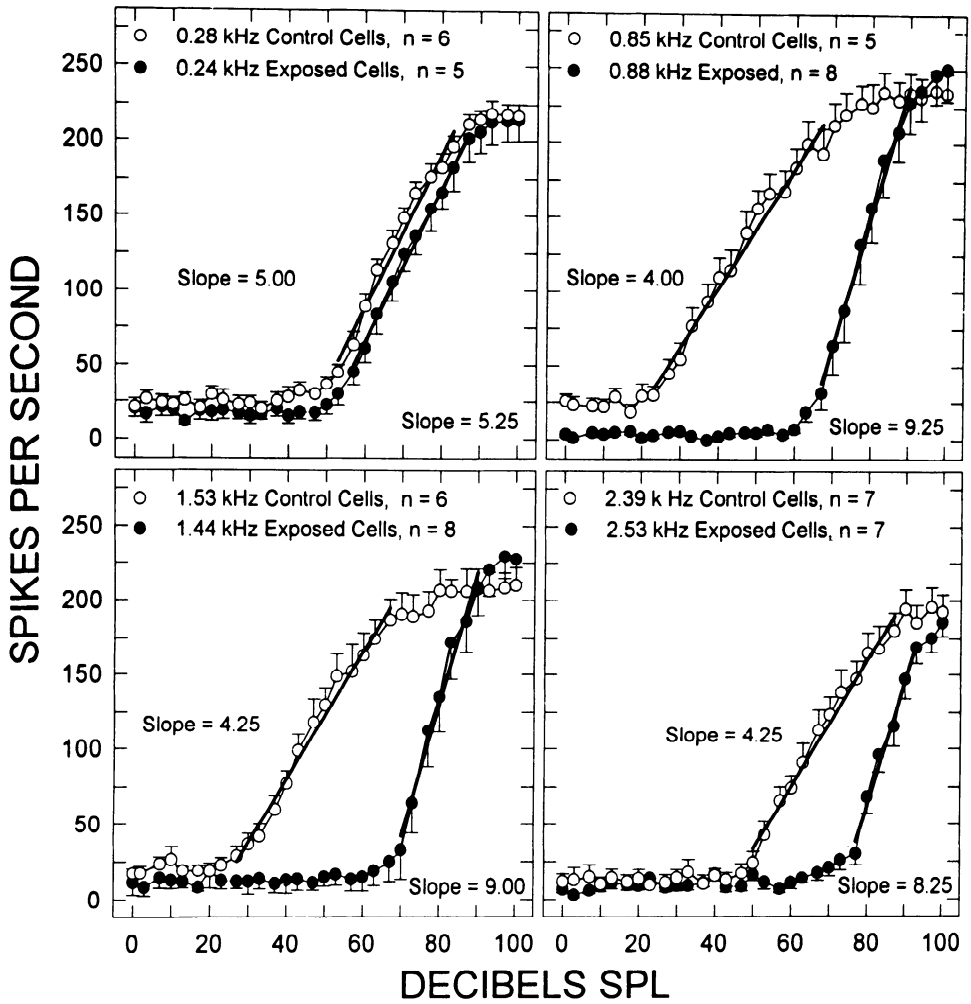

FIG. 12. Rate-intensity functions for control and 0-day recovered cells at 4 different frequency regions. The threshold shift and change in growth rate of the exposed cells are easily identified. Note that the spike rate at saturation is the same in both groups.

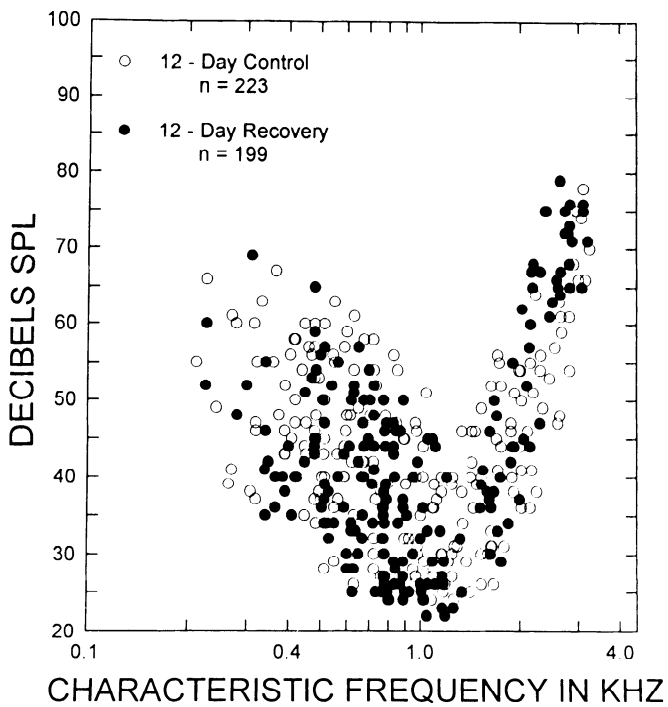

FIG. 13. CF thresholds in 12-day control and recovered cells. The cells in both groups overlap each other.

hair cells an additional 4–6 days to mature (Cotanche and Sulik 1984; Tilney et al. 1986, 1988, 1992). Recent work with adult quails suggested that the new hair cells become reinnervated with an appropriate compliment of afferent and efferent fibers by 10 days postexposure (Ryals and Westbrook 1994).

The nature of acoustic damage to the chick papilla presents a problem. If the primary afferent sensory cells of the papilla remained largely intact, even in the vicinity of the patch and stripe lesions, what then accounts for the initial loss in auditory function and its recovery? A number of possibilities might be considered. *1*) The hair cells lost at the limbic edge of the papilla might play a more important role in cochlear function than thought, or there might be more extensive or subtle damage to the tall hair cells than currently recognized. With regard to these possibilities, there is no reason to expect that the hair cells at the limbic edge of the papilla play a special role in the chick cochlea (Fisher 1994), and although the short and tall hair cells outside of the lesions remain to be systematically explored, the available evidence suggests that at least the sensory hair bundles of these receptor cells appear normal (Cotanche 1987b; Cotanche et al. 1987, 1994; Henry et al. 1988; Marsh et al. 1990; Raphael 1993). *2*) There might be extensive damage in the afferent nerve supply to both tall and short hair cells in the lesion areas, and despite the apparent survival of the tall hair cells, afferent input to the brain stem might be significantly

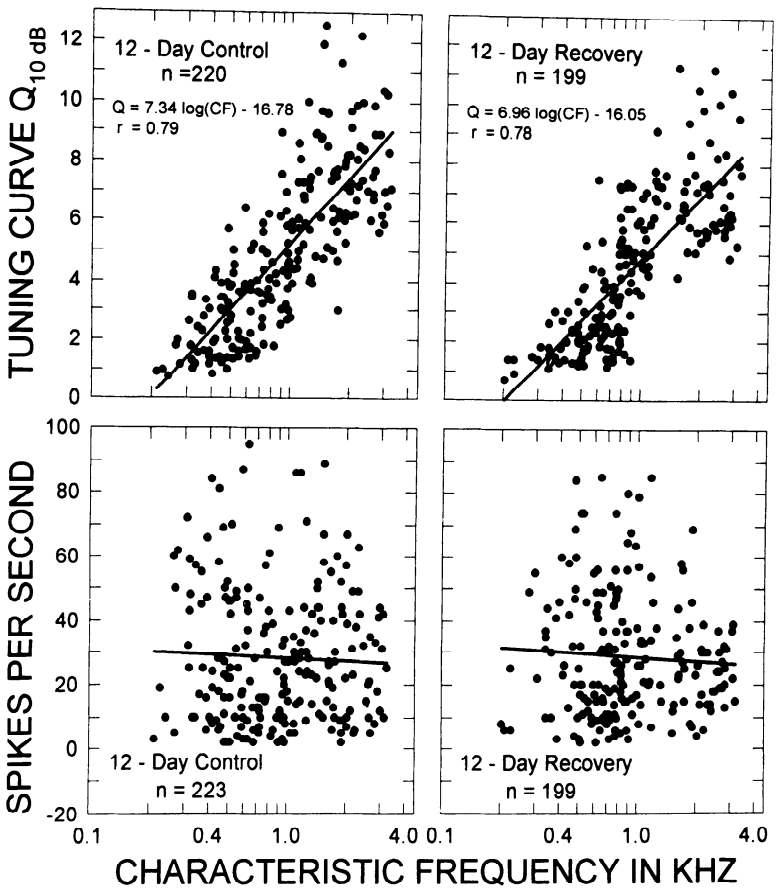

FIG. 14. *Top*: comparison of $Q_{10\ dB}$ values in the 12-day control and recovered groups. *Bottom*: similar comparison for spontaneous activity. A regression line is fit to the data in each panel. The results show complete recovery of these parameters.

curtailed. However, the innervation of surviving hair cells, at least in the quail, appeared normal (Ryals et al. 1992), and only after a postexposure delay of months was loss of cochlear nerve fibers or ganglion cells demonstrated (Ryals et al. 1989). *3*) Short hair cell loss in the patch lesion might significantly contribute directly or indirectly to cochlear nerve afferent activity. It seems unlikely, however, that the missing short hair cells in the patch lesion could account directly for the massive reduction in neural activity, because these cells provided only a small portion of the afferent input to the brain stem (Fisher 1992, 1994). Besides, it is important to realize that 60–70% of the short hair cells in the patch survived the exposure (Marsh et al. 1990). Alternatively, the short hair cells might perform some sort of regulatory function on the tall hair cells analogous to that ascribed to mammalian outer hair cells (Brix and Manley 1994). However, this possibility has yet to be demonstrated. *4*) The cochlear ionic environment might be altered, with a considerable impact on cochlear function. This possibility has some empirical support, because acoustic damage to tegmentum vasculosum in quail has been described (Ryals et al. 1995). Moreover, the endocochlear potential was reduced in chick after overstimulation (Poje et al. 1995). The endocochlear potential is thought to facilitate ion entry into the hair cell transduction channels during stimulation (Hackney and Furness 1995), and a reduction in this potential might impair hair cell depolarization and diminish sound-driven activity in the cochlear nerve (Sewell 1984; Vossieck et al. 1991). The loss and recovery of damage to the (quail) tegmentum vasculosum and (chick) endocochlear potential were well correlated with the loss and recovery (within 3 days) of auditory function (Poje et al. 1995; Ryals et al. 1995). *5*) Finally, the lesion may change cochlear mechanics in such a way that input to the tall hair cell stereocilia is reduced. Saunders and colleagues (Saunders et al. 1992, 1996) have speculated that up-and-down motion of the basilar membrane may be transmitted through the short hair cell stereocilia to the tectorial membrane. This motion is then translated into radial movements of the tectorial membrane over the superior fibrocartilagenous plate. The drawing in Fig. 16*B* suggests that this radial motion would cause a shearing action between the tectorial membrane and the reticular surface of the papilla, thus stimulating tall hair cell stereocilia. This proposed mechanism of tall hair cell stimulation is purely hypothetical, but gains credence when the details of acoustic damage to the basilar papilla are considered.

Tectorial membrane destruction in the patch lesion (Cotanche 1987b, 1992; Cotanche and Dopyera 1990; Cotanche and Picard 1992) occurs over the mobile portion of the papilla and may disrupt the mechanical pathway that stimulates the stereocilia on tall hair cells. This possibility is illustrated in Fig. 16*C*.

There are several pieces of experimental evidence supporting this idea, and admittedly they are indirect. First, significant functional recovery occurs within 3 days postexposure (McFadden and Saunders 1989; Pugliano et al. 1993a,b), which is before the appearance, maturation, or reinnervation of the newly emerging short hair cells (as noted above). The major structural change on the papilla

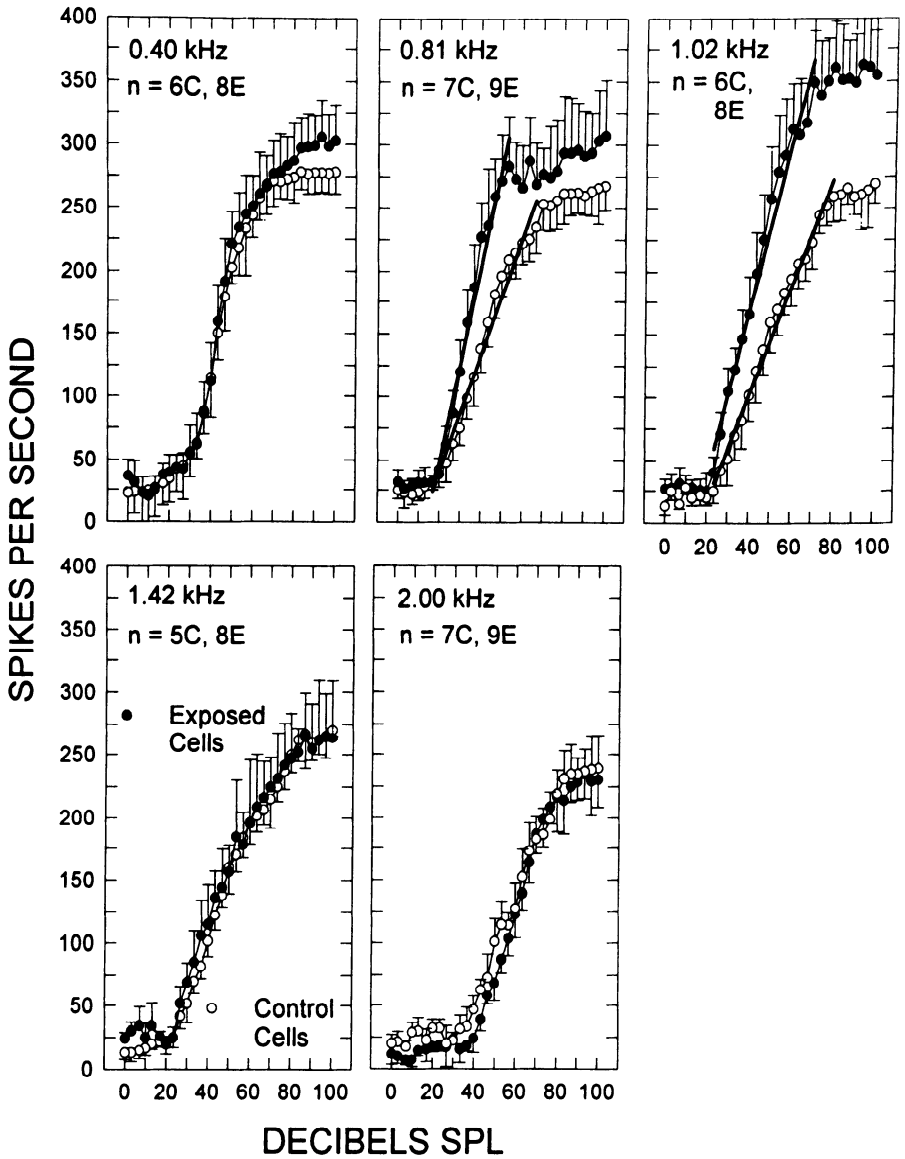

FIG. 15. Rate-intensity functions for 12-day control and recovered cells at different frequencies. All the panels indicate that the threshold for control and exposed cells are the same. The functions at 0.81 and 1.02 kHz indicate an abnormally rapid rate of response growth, with the spike rate exceeding the saturation level of the control cells. Outside of this frequency range the rate-intensity functions appear to be more similar for control and recovered conditions.

surface during these first 3 days is the reappearance of the lower layer of the tectorial membrane and its rearticulation with the remnant of the surviving tectorial membrane (Cotanche 1992; Cotanche and Picard 1992). Figure 16*D, left,* illustrates the appearance of the lower (honeycomb) layer of the papilla at 12 days postexposure, whereas the drawing in Fig. 16*D, right,* shows a cross section of the papilla.

Second, the rate of threshold shift recovery was the same after a 48- or 200-h exposure (McFadden and Saunders 1989; Pugliano et al. 1993b; Saunders et al. 1996). Surprisingly, the papilla after the longer exposure appears to be in a lesser state of damage than the papilla after 48 h. There were new short hair cells already repopulating the patch lesion, and the general organization of the sensory surface had a more normal appearance (Pugliano et al. 1993b). The tectorial membrane at the end of both exposures was destroyed over the patch lesion. The restoration of this membrane in the 200-h exposure followed the same time course as in the shorter exposure.

Finally, the rate-intensity functions (Fig. 12) suggested that the tall hair cells may be physiologically normal, but responding to abnormal input. Both 0-day recovered and 0-day control cells showed the same discharge rate at saturation, suggesting that once an adequate level of input stimulation was achieved, the physiology of the hair cell and its attached cochlear nerve behaved normally. The threshold shift and abnormal spike rate are reminiscent of abnormal mechanical input to the hair cell, as proposed by Tonndorf (1980).

All the processes suggested above need to be explored further, and it is premature to dismiss or accept any of them as the only mechanism contributing to changes in cochlear nerve activity. Indeed, it is likely that the lost function arises from the interplay of several or all of these possibilities.

Frequency-dependent and -independent loss

The 0-day recovered data show a distinction between frequency-dependent and -independent changes in function. It is logical to expect that functional loss should be related to the frequencies coded by the damaged papilla areas. This is certainly true for much of the data reported here. The loss

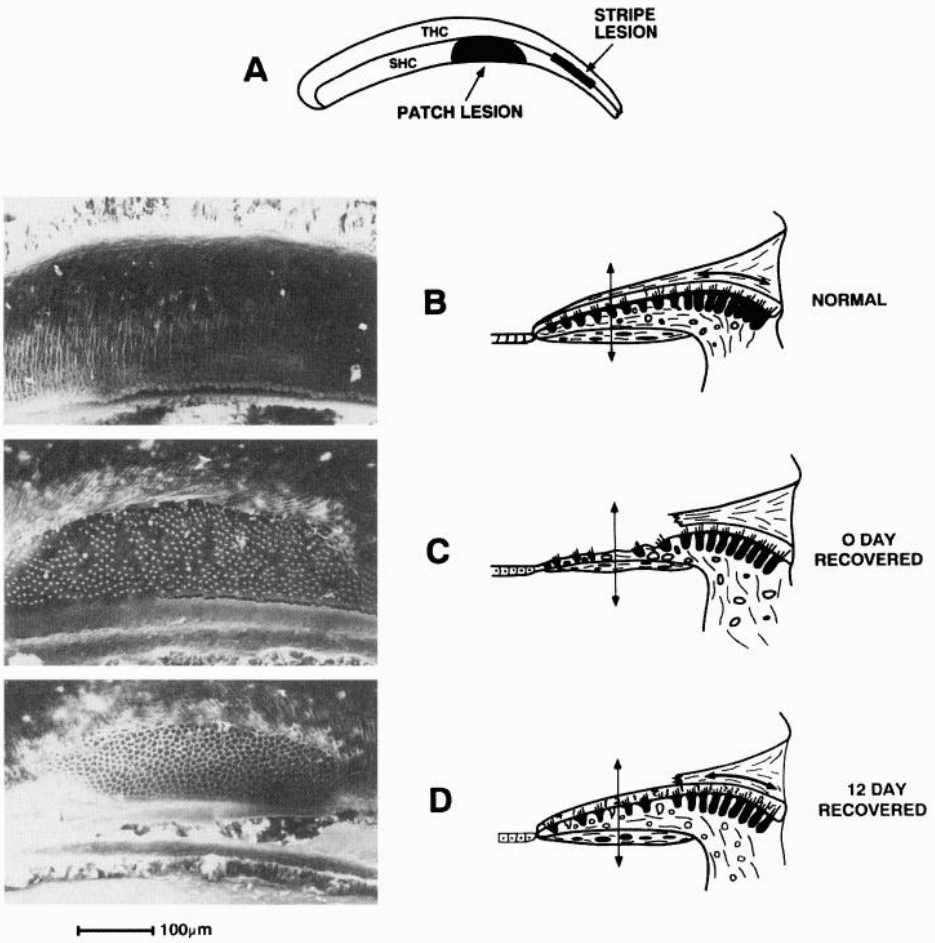

FIG. 16. *A*: regions of the basilar papilla containing tall hair cells (THC) or short hair cells (SHC), as well as the location of the patch lesion and stripe lesions. *B, right*: drawing of the normal cross-sectional appearance of the basilar papilla. Arrows: vertical motion of the papilla above the basilar membrane and radial motion of the tectorial membrane above the tall hair cells. *B, left*: scanning electron microscope view of the papilla surface with the overlying tectorial membrane intact. *C*: drawing and scanning electron microscope pictures show the papilla at 0 days of recovery, and the scattered loss of short hair cells in the patch is apparent. *D*: papilla after 12 days of recovery is illustrated. The scanning electron microscope micrograph shows the regenerated honeycomb layer, and the drawing indicates that the honeycomb is reattached to the old tectorial membrane.

of CF threshold in Fig. 9 was greatest in the frequencies coded by the patch, and the asymmetric loss of CF threshold into the high frequencies could be due to the added effect of the stripe lesion. Similarly, the mid- and high-frequency deterioration in tuning (Fig. 10, *top*) also relates to the patch and stripe areas. Spontaneous activity, however, was reduced throughout the CF spectrum (see Fig. 10, *bottom*). The endocochlear potential data provided by Poje et al. (1995) suggested that the postexposure decrement in this potential was widely distributed throughout scala media. It is worth considering that the altered electrochemical environment in scala media is somehow responsible for reduced spontaneous activity throughout the cochlea. This suggestion must be tempered by the observation that sound-driven activity, at saturation level in the rate-intensity functions, was the same in control and 0-day recovered cells.

Abnormal 12-day rate-intensity functions

Twelve days after the exposure, as noted above, much of the structural damage to the papilla was repaired and the cochlear nerve responses largely returned to normal (Cohen and Saunders 1993; Corwin and Cotanche 1988; Cotanche 1987a; Marsh et al. 1990; McFadden and Saunders 1989). Nevertheless, this functional recovery is accompanied by a glaring defect on the sensory surface in the incompletely recovered tectorial membrane (Fig. 16*D*). The abnormal rate-intensity functions observed in 12-day recovered cells (Fig. 15) present an interesting challenge. Both the growth rates and saturation levels were higher for the 0.8- and 1.0-kHz functions. The fact that the cochlear location normally coding for these frequencies is now occupied by the honeycomb may be important. The problem posed by these functions is to explain how threshold can recover with spike growth rates and saturation levels remaining abnormal. Although we do not know how to account for this peculiar result, one intriguing possibility is that the short hair cell system retains some long-term consequence of acoustic injury beyond the mechanical effects of incomplete tectorial membrane recovery. The short hair cells may have some regulatory effect on tall hair cells, perhaps similar to that between mammalian outer and inner hair cells. Short hair cell damage in the patch area may result in some long-term removal of an inhibitory influence on the tall hair cells. This possibility, of course, needs to be explored further.

Ad referendum

The present results attest to the remarkable ability of the chick ear to recover from acoustic injury. A similar exposure in most, if not all, mammalian ears, would cause a "wipe-out" area in the cochlea, where all hair cells would be completely and permanently destroyed. Structural recovery would not occur, and the sustained damage would be accompanied by a severe or profound hearing loss. Understanding the mechanisms of how acoustic injury is reversed in the

chick ear may provide new insight into the consequences of acoustic injury in the mammalian ear, and perhaps one day may help us understand how to reverse them.

The authors appreciate the critical comments of Dr. Stephen Echteler and K. Duncan, as well as the excellent technical assistance of R. Kurian and P. Schwartz. The editorial work of A. Lieberman is also appreciated.

This research was supported in part by research awards from the National Institute of Deafness and Other Communications Disorders (DC-00710), the Pennsylvania Lions Hearing Research Foundation, and the National Organization for Hearing Research to J. C. Saunders. C. P. Poje was supported by a Newlin Fellowship to the Division of Otolaryngology, Children's Hospital of Philadelphia.

Address for reprint requests: J. C. Saunders, Dept. of Otorhinolaryngology: Head and Neck Surgery, 5-Ravdin-ORL, 3400 Spruce St., Philadelphia, PA 19104.

Received 26 July 1995; accepted in final form 15 March 1996.

REFERENCES

ADLER, H. J., KENEALY, J. F. X., DEDIO, R. M., AND SAUNDERS, J. C. Threshold shift, hair cell loss, and hair bundle stiffness following exposure to 120 and 125 dB pure tones in the neonatal chick. *Acta Otolaryngol.* 112: 444–454, 1992.

ADLER, H. J., POJE, C. P., AND SAUNDERS, J. C. Recovery of auditory function and structure in the chick after two intense pure tone exposures. *Hear. Res.* 71: 214–224, 1993.

BRIX, J. AND MANLEY, G. A. Mechanical and electromechanical properties of the stereociliar bundles of isolated and cultured hair cells of the chicken. *Hear. Res.* 76: 147–157, 1994.

COHEN, Y. E., HERNANDEZ, H. N., AND SAUNDERS, J. C. Middle-ear development. II. Structural development of the chick middle ear. *J. Morphol.* 212: 257–267, 1992a.

COHEN, Y. E., RUBIN, D. M., AND SAUNDERS, J. C. Middle-ear development. I. Extra-stapedius response in the neonatal chick. *Hear. Res.* 58: 1–8, 1992b.

COHEN, Y. E. AND SAUNDERS, J. C. The effects of sound overexposure on the spectral response patterns of nucleus magnocellularis in the neonatal chick. *Exp. Brain Res.* 95: 202–212, 1993.

CORWIN, J. T AND COTANCHE, D. A. Regeneration of sensory hair cells after acoustic trauma. *Science Wash. DC* 240: 1772–1774, 1988.

COTANCHE, D. A. Regeneration of hair cell stereociliary bundles in the chick cochlea following severe acoustic trauma. *Hear. Res.* 30: 181–196, 1987a.

COTANCHE, D. A. Regeneration of the tectorial membrane in the chick cochlea following severe acoustic trauma. *Hear. Res.* 30: 197–206, 1987b.

COTANCHE, D. A. Video-enhanced DIC images of the noise-damaged and regenerated chick tectorial membrane. *Exp. Neurol.* 115: 23–27, 1992.

COTANCHE, D. A. AND CORWIN, J. T. Stereocilia bundles reorient during hair cell development and regeneration in the chick cochlea. *Hear. Res.* 52: 379–402, 1991.

COTANCHE, D. A. AND DOPYERA, C. E. J. Hair cell and supporting cell response to acoustic trauma in the chick cochlea. *Hear. Res.* 46: 29–40, 1990.

COTANCHE, D. A., LEE, K. H., STONE, J. S., AND PICARD, D. A. Hair cell regeneration in the bird cochlea following noise damage or ototoxic drug damage. *Anat. Embryol.* 189: 1–18, 1994.

COTANCHE, D. A. AND PICARD, D. A. Progression of damage to the chick tectorial membrane with increased length of noise exposure. *Abstr. Assoc. Res. Otolaryngol.* 15: 116, 1992.

COTANCHE, D. A., SAUNDERS, J. C., AND TILNEY, L. G. Hair cell damage produced by acoustic trauma in the chick cochlea. *Hear. Res.* 25: 267–286, 1987.

COTANCHE, D. A. AND SULIK, K. K. The development of stereociliary bundles in the cochlear duct of chick embryos. *Dev. Brain Res.* 16: 181–193, 1984.

DOLAN, D. F., TEAS, D. C., AND WALTON, J. P. Postnatal development of physiological responses in auditory nerve fibers. *J. Acoust. Soc. Am.* 78: 544–554, 1985.

EVANS, E. F. AND NELSON, P. G. The response of single neurons in the cochlear nucleus of the cat as a function of their location and anesthetic. *Exp. Brain Res.* 17: 402–407, 1973.

FISHER, H. P. Quantitative analysis of the innervation of the chicken basilar papilla. *Hear. Res.* 61: 167–178, 1992.

FISHER, H. P. General pattern and morphologic specializations in the avian cochlea. *Scanning Microsc.* 8: 351–364, 1994.

HACKNEY, C. M. AND FURNESS, D. N. Mechanotransduction in vertebrate hair cells: structure and function in the stereociliary bundle. *Am. J. Physiol.* 268 (*Cell Physiol.* 37): C1–C13, 1995.

HENRY, W. J., MAKARETZ, M. O., SAUNDERS, J. C., SCHNEIDER, M. E., AND VRETTAKOS, P. Age dependent loss and recovery of hair cells in the chick following exposure to intense sound. *Otolaryngol. Head Neck Surg.* 98: 607–611, 1988.

KALTENBACH, J. A. AND SAUNDERS, J. C. Spectral and temporal response patterns of single units in the chinchilla dorsal cochlear nucleus. *Exp. Neurol.* 96: 406–419, 1987.

KETTNER, R. E., FENG, J. Z., AND BRUGGE, J. F. Postnatal development of the phase-locked response to low frequency tones of auditory nerve fibers in the cat. *J. Neurosci.* 5: 275–283, 1985.

MANLEY, G. A., KAISER, A., BRIX, J., AND GLEICH, O. Activity pattern of primary auditory-nerve fibers in chickens: development of fundamental properties. *Hear. Res.* 57: 1–15, 1991.

MARSH, R. R., XU, L., MOY, J. P., AND SAUNDERS, J. C. Recovery of the basilar papilla following intense sound exposure in the chick. *Hear. Res.* 46: 229–238, 1990.

MCFADDEN, E. A. AND SAUNDERS, J. C. Recovery of auditory function following intense sound exposure in the neonatal chick. *Hear. Res.* 41: 205–216, 1989.

POJE, C. P., SEWELL, D. A., AND SAUNDERS, J. C. The effects of exposure to intense sound on the DC endocochlear potential in the chick. *Hear. Res.* 82: 197–204, 1995.

PUGLIANO, F. A., PRIBITKIN, E., ADLER, H. J., AND SAUNDERS, J. C. Growth of evoked potential amplitude in neonatal chicks exposed to intense sound. *Acta Otolaryngol.* 113: 18–25, 1993a.

PUGLIANO, F. A., WILCOX, T., ROSSISTER, J., AND SAUNDERS, J. C. Recovery of auditory structure and function in neonatal chicks exposed to intense sound for eight days. *Neurosci. Lett.* 151: 214–218, 1993b.

RAPHAEL, Y. Damage to the tectorial membrane may protect chick hair cells from noise overstimulation. *Hear. Res.* 53: 173–184, 1991.

RAPHAEL, Y. Evidence for supporting cell mitosis in response to acoustic trauma in the avian ear. *J. Neurocytol.* 21: 663–671, 1992.

RAPHAEL, Y. Reorganization of the chick basilar papilla after acoustic trauma. *J. Comp. Neurol.* 330: 521–532, 1993.

ROMAND, R. Functional properties of auditory-nerve fibers during postnatal development in the kitten. *Exp. Brain Res.* 56: 395–402, 1984.

ROSE, J. E., HIND, J. E., ANDERSON, D. J., AND BRUGGE, J. F. Some effects of stimulus intensity on response of auditory nerve fibers in the squirrel monkey. *J. Neurophysiol.* 34: 685–699, 1971.

RYALS, B. M., STALFORD, M. D., LAMBERT, P. R., AND WESTBROOK, E. W. Recovery of noise-induced changes in dark cells of the quail tegmentum vasculosum. *Hear. Res.* 83, 51–61, 1995.

RYALS, B. M., TEN EYCK, B., AND WESTBROOK, E. W. Ganglion cell loss continues after hair cell regeneration. *Hear. Res.* 43: 81–90, 1989.

RYALS, B. M. AND WESTBROOK, E. W. TEM analysis of neural terminals on autoradiographically identified regenerated hair cells. *Hear. Res.* 72: 81–88, 1994.

RYALS, B. M., WESTBROOK, E. W., STOOTS, S., AND SPENCER, R. F. Changes in the acoustic nerve after hair cell regeneration. *Exp. Neurol.* 115: 18–22, 1992.

SALVI, R. J., SAUNDERS, J. C., HASHINO, E., AND CHEN, L. Discharge patterns of chicken cochlear ganglion neurons following kanamycin induced hair cell loss and regenerations. *J. Comp. Physiol. A Sens. Neural Behav. Physiol.* 174: 351–369, 1994.

SALVI, R. J., SAUNDERS, S. S., POWERS, N. L., AND BOETTCHER, F. A. Discharge patterns of cochlear ganglion neurons in the chicken. *J. Comp. Physiol. A Sens. Neural Behav. Physiol.* 170: 227–241, 1992.

SAUNDERS, J. C., ADLER, H. J., AND PUGLIANO, F. A. The structural and functional aspects of hair cell regeneration in the chick as a result of exposure to intense sound. *Exp. Neurol.* 115: 13–17, 1992.

SAUNDERS, J. C., DOAN, D. E., COHEN, Y. E., ADLER, H. J., AND POJE, C. P. Recent observations on the recovery of structure and function in the sound-damaged chick ear. In: *Auditory Plasticity and Regeneration: Scientific and Clinical Implications,* edited by R. J. Salvi, D. Henderson, F. Fiorino, and V. Colletti New York: Thieme, 62–83, 1996.

SAUNDERS, J. C., RELKIN, E. M., ROSOWSKI, J. J., AND BAHL, C. Changes in middle-ear input admittance during postnatal auditory development in chicks. *Hear. Res.* 24: 227–235, 1986.

SAUNDERS, J. C., TORSIGLIERI, A., AND DEDIO, R. The growth of hearing loss in neonatal chicks exposed to intense pure tones. *Hear. Res.* 69: 25–34, 1993.

SCHWARTZKOPFF, J. AND BREMOND, J. Méthode de dérivation des potentials cochléailes chex l'oiseau. *J. Physiol. Paris* 55: 495–518, 1963.

SEWELL, W. F. The effects of furosemide on the endocochlear potential and auditory-nerve fiber tuning curves in cats. *Hear. Res.* 14: 305–314, 1984.

SMITH, C. A. Inner ear. In: *Form and Function in Birds,* edited by A. S. King and J. McLelland. New York: Academic, 1985, p. 237–310.

STONE, J. S. AND COTANCHE, D. A. Synchronization of hair cell regeneration in the chick cochlea following noise damage. *J. Cell Sci.* 102: 671–680, 1992.

TAKASAKA, T. AND SMITH, C. A. The structure and innervation of the pigeon's basilar papilla. *J. Ultrastruct. Res.* 35: 20–65, 1971.

TANAKA, A AND SMITH, C. A. Structure of the chicken's inner ear: SEM and TEM study. *Am. J. Anat.* 153: 251–272, 1978.

TILNEY, L. G., COTANCHE, D. A., AND TILNEY, M. S. Actin filaments, stereocilia and hair cells of the bird cochlea. VI. How the number and arrangement of stereocilia are determined. *Development* 116: 213–226, 1992.

TILNEY, L. G., TILNEY, M. S., AND COTANCHE, D. A. Actin filaments, stereocilia, and hair cells of the bird cochlea. V. How the staircase pattern of stereocilia length is generated. *J. Cell Biol.* 106: 355–365, 1988.

TILNEY, L. G., TILNEY, M. S., SAUNDERS, J. C., AND DE ROSIER, D. J. Actin filaments, stereocilia, and hair cells of the bird cochlea. III. The development and differentiation of hair cells and stereocilia. *Dev. Biol.* 116: 100–118, 1986.

TONNDORF, J. Acute cochlear disorders: the combination of hearing loss, recruitment, poor speech discrimination, and tinnitus. *Ann. Otol.* 89: 353–358, 1980.

VOSSIECK, T., SCHERMULY, L., AND KLINKE, R. The influence of DC polarization of the endocochlear potential on single fibre activity in the pigeon cochlear nerve. *Hear. Res.* 56: 93–100, 1991.

WALSH, E. J. AND MCGEE, J. Postnatal development of auditory nerve and cochlear nucleus neuronal responses in kittens. *Hear. Res.* 28: 97–116, 1987.

WARCHOL, M. E. AND DALLOS, P. Neural coding in the chick cochlear nucleus. *J. Comp. Physiol. A Sens. Neural Behav. Physiol.* 166: 721–734, 1990.